Thermodynamic Analysis of a Direct Air Carbon Capture Plant with Directions for Energy Efficiency Improvements

by

Ryan M. Long-Innes
B.Eng., University of Victoria, 2020

A Thesis Submitted in Partial Fulfillment of the Requirements for the Degree of

MASTER OF APPLIED SCIENCE

in the Department of Mechanical Engineering

Thermodynamic Analysis of a Direct Air Carbon Capture Plant with Directions for Energy Efficiency Improvements

by

Ryan M. Long-Innes
B.Eng., University of Victoria, 2020

Supervisory Committee

Dr. Henning Struchtrup, Supervisor
(Department of Mechanical Engineering)

Dr. Andrew Rowe, Committee Member
(Department of Mechanical Engineering)

Dr. Curran Crawford, Committee Member
(Department of Mechanical Engineering)

Abstract

According to the Intergovernmental Panel on Climate Change, Carbon Dioxide Removal (CDR) technologies play a significant role in deep mitigation pathways to limit global temperature rise to 1.5°C. As a result, interest in them is becoming increasingly prevalent, the most widely discussed being Direct Air Capture (DAC), or active removal of carbon dioxide from atmospheric air.

While DAC processes have indeed been successfully tested, one of the most prominent being that developed by Canadian company Carbon Engineering, their widespread deployment faces significant headwinds due to prohibitively high energy consumption and its associated costs. Before DAC can be considered to exist in a state of technological readiness, reductions to the installations' energy demand must be realized.

This thesis analyzes the thermodynamic behavior of Carbon Engineering's proposed 1 Mt-CO_2/year natural gas fuelled DAC plant, which they describe as "a low-risk starting point rather than a fully optimized least-cost design" [Keith et al., Joule **2**, 1573], with the aim to illustrate key areas to which energy efficiency improvement measures must target. With an understanding built of the mechanisms by which energy is utilized and irreversibly lost within their plant, suggestions are put forth for directions to pursue for process improvements, with further analysis included on potential alternative plant configurations which would reduce overall heat and power consumption.

A thermodynamic work loss analysis is performed on their plant design at a system level, which finds 92.2% of incoming exergy being lost to thermodynamic irreversibilities. A component-level analysis is then performed to detail the mechanisms by which these losses occur in the most energy-intensive plant segments, namely, the calciner and preheat cyclones, air separation unit, water knockout system, CO_2 compression system, and power island. The dissipation of chemical exergy in the air contactor component, i.e., the release of stored chemical exergy as low-grade heat to the environment due to the exothermic reaction of CO_2 and aqueous KOH, was determined as the largest unavoidable source of work loss. The most avoidable losses were found to be associated with use of natural gas as a feedstock for heat and power, namely, through its introduction of additional CO_2 and water to be processed within the plant, and due to gas turbine power production's inherent Carnot efficiency limits.

Additional analysis and discussion follows regarding possible loss reduction measures and modifications, the key concept presented being the use of renewable energy to provide plant power, combined with a calciner using electric resistance heating to meet its reduced thermal demand. Use of a readily-available high-temperature heat source for calciner heat is also considered, with thorough description included of its thermodynamic advantages. Finally, the all-electric plant concept is analyzed at a system level, and its advantages compared to the original natural gas fuelled case.

Table of Contents

List of Figures

List of Tables

Acknowledgements

I would like to extend special thanks to my friend and graduate supervisor, Henning Struchtrup, for his unending support of my academic and career endeavors. It is thanks to you that I became interested in the fascinating concepts of thermodynamics and energy conversion, along with their formidable applications in the modern world. For this, I will always be grateful.

I would also like to thank Curran Crawford and Andrew Rowe for their invaluable advice, intellectual support, and feedback throughout the course of my studies. I also thank the Pacific Institute for Climate Solutions and the Solid Carbon project team for their input and eager willingness to exchange ideas, all of which led to highly engaging discussions. Finally, the financial support I received throughout my graduate studies from NSERC and the University of Victoria was greatly appreciated.

Chapter 1
Introduction

Since the beginning of the industrial revolution, fossil fuels have consistently met humanity's energy requirements due to their high energy density, global abundance, convenience and ease of use. As they are burned, their common combustion product, carbon dioxide (CO_2), is released to the earth's atmosphere. As humanity's demand for energy has increased year over year, so have emissions of CO_2, increasing by ~134 ppm overall above pre-industrial levels as of August 2021 [2][3]. Due to its greenhouse (or 'heat-trapping') properties, its consistent emission in increasingly large quantities has the unintended consequence of rapidly disrupting the earth's energy balance and natural climate cycles, posing uncertain and potentially grave risks to the planet's environmental stability and future human society [4]. Thus, international efforts are underway to curb the use of fossil fuels, minimize further emissions of greenhouse gases such as CO_2, and in doing so, limit the rise in average global temperature.

By analysis of IPCC Integrated Assessment Models, Carbon Dioxide Removal (CDR) technologies, i.e., ones which actively remove CO_2 from the atmosphere, were found to play significant roles in all scenarios in which 1.5°C to 2°C temperature targets are reached, with most removal estimates ranging between 5 to 15 Gt-CO_2/year by 2050 [5]. The National Academies of Sciences, Engineering and Medicine estimate 10 Gt-CO_2/year by 2050, and 20 Gt-CO_2/year by 2100, to meet Paris Agreement targets without significant detriment to global economic growth [6].

Various methods have been proposed to decrease atmospheric CO_2 content, some of which include afforestation and reforestation, ocean alkalinity enhancement, biomass energy with carbon capture and storage (BECCS), and Direct Air Capture (DAC) [5].

Direct Air Capture plants, such as that proposed by the Canadian company Carbon Engineering [1], are designed to actively remove carbon dioxide from atmospheric air. The general process involves drawing large amounts of air through a 'contactor', in which its CO_2 molecules bind with a solid sorbent or liquid solvent material, recovering the bound CO_2 in a concentrated stream, then pumping said stream out of the plant for permanent storage or industrial use [7][8].

While DAC processes are technologically sound, i.e., they do in fact provide negative emissions, it could be argued that their energy usage is prohibitively excessive for large-scale deployment – based on Carbon Engineering's published data, with their plant consuming 8.81 GJ of natural gas per ton of CO_2 captured [1], and at their capture rate of 111.9 t-CO_2/h, removal of 10 Gt-CO_2/year [6] would require consumption of ~58% of 2019's global natural gas production [9]. As a result, improvements to the process, either to its underlying chemical cycles or to its internal usage of heat and power, become a necessity before the technology can be considered ready for widespread deployment.

Thus, the motivation for this thesis is to provide an in-depth analysis and discussion of how energy is used within Carbon Engineering's plant, how much of it is lost to thermodynamic irreversibilities, the extent to which these losses are avoidable, and the means by which they may be reduced. The data presented and the conclusions reached may then serve as a guide for development of improved DAC processes, and future work may determine the efficacy, practicality, and financial feasibility of the improvements suggested.

Chapter 2 presents a research paper as it was submitted for publication [10], less the abstract, detailing an analysis of the Carbon Engineering plant's losses to thermodynamic irreversibilities and the

mechanisms by which they occur. From this analysis, an understanding is built of how energy is consumed and lost throughout the plant, and discussion follows of possible directions to pursue for process improvements.

Based on the results and suggestions of Chapter 2, more formal analysis of possible improvements to the Calciner system, the largest consumer of energy in the plant and driver of significant irreversible losses, follows in Chapter 3. Analysis and discussion is presented on its thermodynamic behavior, on use of thermal versus work resources to meet its energy demand, and on the thermodynamic implications of replacing natural gas use with electric power. Chapter 4 then uses these results to analyze a theoretical alternative plant configuration at a system level, determining its expected power consumption, its net work loss to entropy generation, and its second law efficiency with respect to power supplied.

Finally, all key results are summarized in the Summary and Conclusion section, and with them the implications for DAC process improvements and large-scale deployment.

Chapter 2

Research Paper: 'Thermodynamic Loss Analysis of a Liquid-Sorbent Direct Air Carbon Capture Plant'

The contents of this chapter is taken directly from the aforementioned research paper submitted for publication. Entitled 'Thermodynamic Loss Analysis of a Liquid-Sorbent Direct Air Carbon Capture Plant' [10], its main author is also the author of this thesis, having done its research, calculations and writing in consultation with Dr. Henning Struchtrup as advisor. The paper includes system-level and component-level thermodynamic work loss analyses of Carbon Engineering's 1 Mt-CO_2/year DAC plant, with discussion following on directions for plant improvements based on the data obtained. All section, equation, and reference numbering has been modified to integrate it with this thesis.

2.1 Introduction and Background

According to studies from the Intergovernmental Panel on Climate Change, Carbon Dioxide Removal (CDR) technologies play significant roles in all pathways examined to limit global temperature rise to 1.5°C [4]. As global CO_2 emissions continue to rise, interest in technologies designed to actively remove the gas from the atmosphere is becoming increasingly prevalent. One of the most promising of these negative-emissions technologies under development, known as Direct Air Capture (hereafter referred to as DAC), uses solid-sorbent or aqueous-sorbent filters to sequester carbon dioxide directly from atmospheric air. The CO_2 may subsequently be pumped underground for permanent geological storage, or used for various industrial and chemical processes, production of synthetic hydrocarbon fuels, or enhanced oil recovery [8].

DAC, while appearing to be a promising technology, faces many challenges. With the amount of CO_2 in atmospheric air being very dilute, DAC requires massive amounts of energy per unit of CO_2 captured, incurring significant energy costs in processing large volumes of air and in regeneration of the sorbent material. Partly as a result of this high energy demand, it becomes a rather cost-intensive process.

The Canadian company Carbon Engineering has proposed an aqueous-sorbent based chemical looping process for DAC, capable of capturing 0.98 Mt-CO_2/year (111.9 t-CO_2/h) [1]. For our analysis, their plant design was selected due to its scalability and its publicly available process data. A simplified schematic of their natural gas-powered ('A' Configuration [1]) plant design is shown in Figure 2.1. A more detailed plant schematic, as was used for process analysis in this paper, is presented in Ref. [1].

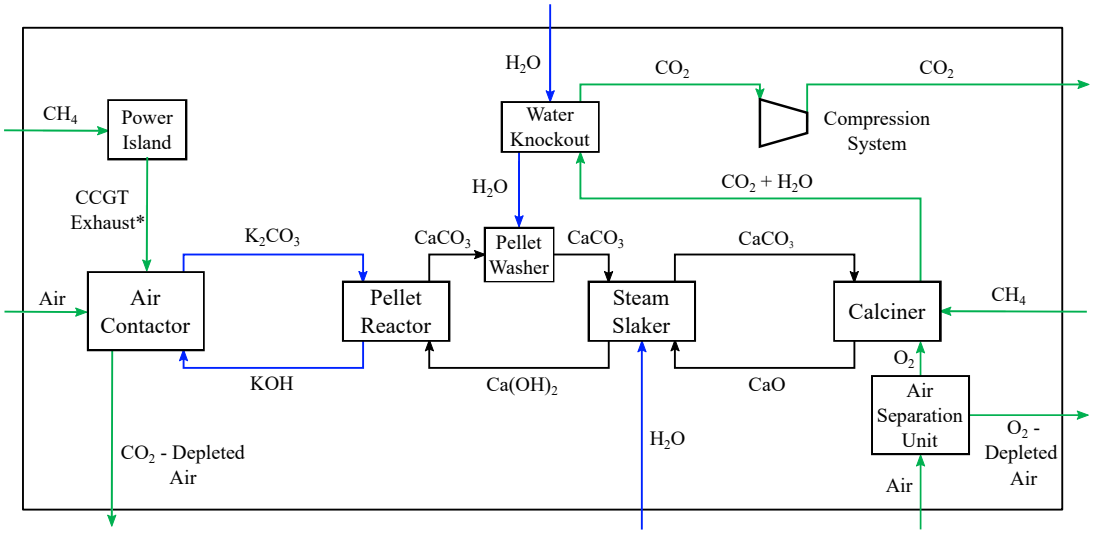

Figure 2.1: Simplified Process Schematic of Carbon Engineering's 1 Mt-CO_2/year DAC Plant (see Ref. [1]), indicating Main Material and Chemical Flows

*Exhaust gas from the CCGT system passes through a separate CO_2 Absorber (coupled to the Pellet Reactor's KOH loop) to partially capture its CO_2 content prior to its passage through the Air Contactor [1]. We omit it here for illustrative purposes.

The process begins with atmospheric air being drawn by large fans into the Air Contactor, in which it is exposed to sorbent material wetted with potassium hydroxide (KOH) in solution. The air's CO_2 content reacts with the potassium hydroxide to yield potassium carbonate (K_2CO_3) and water, forming an aqueous solution.

This solution is then passed to a Pellet Reactor in which it is precipitated with calcium hydroxide ($Ca(OH)_2$) to form solid pellets of calcium carbonate ($CaCO_3$) along with potassium hydroxide (KOH) for re-use. The calcium carbonate pellets are washed to remove residual KOH, partially pre-heated by the Steam Slaker, and finally transported to the Calciner: here, CO_2 is released from calcium carbonate through calcination, i.e., heat input at high temperature, through oxy-fuel combustion of natural gas (primarily CH_4) with 95.60% pure oxygen gas, the oxygen being provided by a cryogenic Air Separation Unit (ASU). Lime, or calcium oxide (CaO), being the other product of calcination, is slaked with water in the Steam Slaker to produce calcium hydroxide for the Pellet Reactor, hence completing Carbon Engineering's chemical loop system.

A portion of the water vapor in the Calciner's outgoing gas stream, produced as a combustion product, is removed via the Water Knockout drum, the remainder being removed in the four-stage Compression System's intercooling stages. The concentrated CO_2 stream then leaves the Compression System (and plant) at 151 bar [1].

In Figure 2.1, the Power Island encompasses a Combined Cycle Gas Turbine (CCGT) system and steam turbine integrated with the plant's major components, i.e., the gas turbine exhaust's CO_2 is also absorbed in KOH solution, while the steam turbine is fed with both Slaker and HRSG steam superheated through heat exchange with the Calciner's outgoing gas stream.

Carbon Engineering estimates net levelized cost to range between (2016 USD) \$94-232/t-CO_2 captured from the atmosphere, the lower value assuming a 7.5% Capital Recovery Factor with natural gas and grid electricity used to produce CO_2 at 0.1 MPa, the upper assuming 12.5% CRF with an electrically neutral plant (only natural gas used for energy) producing pipeline-ready CO_2 at 15 MPa [1].

According to the 2019 committee report published by the National Academies of Sciences, Engineering and Medicine, to meet Paris Agreement targets for atmospheric greenhouse gas reduction [11] without significant detriment to global economic growth, carbon removal technologies such as DAC will need to remove 10 Gt-CO_2/year from the atmosphere by 2050, and 20 Gt-CO_2/year by 2100 [6]. By simple calculation using Carbon Engineering's levelized cost range, removal of these amounts using their technology would correspond to a net cost range of \$940B - \$2.32T/year by 2050, or \$1.88T - \$4.62T/year by 2100 (in 2016 US dollars). For comparative purposes, using CPI inflation-adjusted [12] costs of \$85-211/t-CO_2 with 2010 US dollars as a baseline (due to available GDP data [13]), this amounts to 1.0% - 2.5% of 2019's global real GDP of \$84.97T (2010 USD) [13] by 2050, or 2.0% - 5.0% by 2100.

Carbon Engineering's calculations assume a fixed natural gas cost of \$3.50/GJ [1] - for their baseline 'A' (natural gas) configuration, with gas input at 8.81 GJ/t-CO_2, energy input accounts for \$30.84/t-CO_2. For their lowest-cost configuration, gas input at 5.25 GJ/t-CO_2 accounts for \$18.38/t-CO_2 and grid electricity, priced between \$30-\$60/MWhr, accounts for \$2.31 - \$4.62/t-CO_2. At the 2050 removal rate target, with their existing technology, their 'A' configuration would require a natural gas input of 8.81×10^{10} GJ/year (2.36T Nm^3/year), or 58% of 2019's global natural gas production of 4.089T Nm^3 [9]. Such massive demand would certainly increase the price of the commodity, and would present tremendous logistical challenges to widespread deployment.

With energy costs contributing significant portions to the net cost of capture, and because energy consumption in the existing design could be argued to be prohibitive to large-scale deployment, in this report we identify the segments of the plant in which the largest work losses due to irreversibilities occur, i.e., the primary system components which energy efficiency improvement measures must target. Section 2.3 presents a system-level analysis in which the plant's net overall work loss and second-law efficiency are quantified. Analysis of individual components then follows in Section 2.4, wherein we discuss the reasons and mechanisms by which these losses occur. Finally, in Sections 2.5 and 2.6, we summarize our results and discuss their implications for large-scale implementation of Direct Air Capture technology, including brief estimates of energy consumption when substituting natural gas with renewable energy sources.

2.2 Methods

Thermodynamic analysis of Carbon Engineering's 1 Mt/yr plant was performed by applying mass, energy and entropy balances over each relevant component or subsystem, with Carbon Engineering's published simulation results [1] providing known quantities where necessary. Wolfram Mathematica and MathWorks' MATLAB software were used to solve the equations – because they keep track of all variables in use, computed outflows from one subsystem could be applied as inflows to another, and a general picture of energy consumption and subsystems' losses to irreversibilities could be obtained without use of specialized simulation software.

Shomate equations were used to calculate the majority of heat capacity, enthalpy and entropy values used in MATLAB and Mathematica, their use being deemed sufficiently accurate when the ideal gas equation was satisfied to at least 95% accuracy (i.e., for any species in question, $pv/RT > 0.95$). All Shomate constants and other thermochemical data (molar masses, standard enthalpies, standard entropies) were obtained from the NIST Chemistry WebBook [14], with the exception of $CaCO_3$, where published data by Jacobs et al. [15] was used, and water vapor < 500 K, whose Shomate constants were obtained from Ref. [16]. The enthalpy reference point for all chemical species was chosen as their enthalpy of formation at standard conditions (1 bar, 298.15 K).

Where Shomate equations/ideal gas assumptions were not sufficiently accurate (pv/RT < 0.95), or when water occurred in a liquid state, thermophysical properties were calculated from a MATLAB implementation of the IAPWS IF-97 standard [17] for water and steam, while CO_2 properties at high pressures were calculated from a similar implementation of Span and Wagner's Equation of State for CO_2 [18].

For all cases presented, balance equations assume steady-state operation of the plant; i.e., all time derivatives vanish. Energy balances neglect changes in kinetic and potential energy, considering only enthalpic differences between incoming and outgoing chemical species flows to have an effect on rates of work and heat exchange.

The mass, energy and entropy balances thus all assume the respective forms [19]

$$\sum_{out} \dot{m}_e = \sum_{in} \dot{m}_i, \tag{2.1}$$

$$\sum_{out} \dot{n}_e \bar{h}_e - \sum_{in} \dot{n}_i \bar{h}_i = \dot{Q}_0 + \sum_k \dot{Q}_k - \dot{W}, \tag{2.2}$$

$$\sum_{out} \dot{n}_e \bar{s}_e - \sum_{in} \dot{n}_i \bar{s}_i - \frac{\dot{Q}_0}{T_0} - \sum_k \frac{\dot{Q}_k}{T_k} = \dot{S}_{gen} \geq 0, \tag{2.3}$$

where $\dot{m}$ denotes mass flow rate, $\dot{n}$ mole flow rate, $\bar{h}$ molar specific enthalpy, $\bar{s}$ molar specific entropy, $\dot{W}$ rate of work (power), $\dot{Q}_k$ heat transfer rate over a system boundary at temperature T_k, and $\dot{S}_{gen}$ the rate of entropy generation in the system. These equations are valid for all open systems and subsystems considered in our analysis.

For any variable x, we use the notation $\dot{x}$ to represent its rate of change with time, e.g., a time-invariant quantity of work is denoted W, while rate of work (power) is denoted $\dot{W}$. Because we rarely speak in terms of time-invariant quantities throughout our analysis, terms such as *work potential*, *reversible work* and *work loss* often refer to rates of work. To avoid confusion when discussed, time-invariant quantities of work and heat will always be preceded with qualifiers 'mass-specific', 'mole-specific', etc.

Note that in Eqns. (2.2) and (2.3), we isolate a term $\dot{Q}_0$, which is the heat exchange with the external environment at temperature T_0 (we choose 21°C [1]), the environment being considered a freely available heat source/sink. From here, we eliminate $\dot{Q}_0$ between Eqs. (2.2) and (2.3) to find power as

$$\dot{W} = -T_0 \dot{S}_{gen} + \sum_k (1 - \frac{T_0}{T_k}) \dot{Q}_k + \sum_{in} \dot{n}_i (\bar{h}_i - T_0 \bar{s}_i) - \sum_{out} \dot{n}_e (\bar{h}_e - T_0 \bar{s}_e). \tag{2.4}$$

In Eq. (2.4), work loss to irreversibilities is represented by [19]

$$\dot{W}_{loss} = T_0 \dot{S}_{gen} \geq 0, \tag{2.5}$$

where according to our sign convention, $\dot{W}_{loss}$ increases power requirements for power-consuming systems, and decreases power output for power-producing systems.

For fully reversible systems, for which entropy generation $\dot{S}_{gen}$ vanishes, Eq. (2.4) gives the minimum possible power requirement ($\dot{W} < 0$) for power-consuming components/systems, or the highest possible power output ($\dot{W} > 0$) for power producing systems, i.e., thermodynamically reversible work.

Overall, in irreversible thermodynamic processes, entropy is generated, reducing the efficiency of energy conversion. In the context of the systems we analyze, irreversibilities primarily occur due to

undesired heat transfer, uncontrolled chemical reactions, mixing of chemical streams, and friction.

Eq. (2.4) can also be written as

$$\dot{W} = \dot{W}_{rev} - \dot{W}_{loss} \tag{2.6}$$

where, for the present energy-consuming application, actual work ($\dot{W}$) and reversible work ($\dot{W}_{rev}$) are inputs and are therefore negative, while the loss ($\dot{W}_{loss}$) is a positive quantity such that it increases the actual work required. Depending on the nature and magnitude of irreversibilities, the actual work requirement can be substantially larger than the minimum required, i.e., reversible, work. This is indeed the case for DAC at a system level.

A useful measure for process quality is the Second-Law Efficiency, which measures the ratio between minimum work requirement and actual work requirement in practice, [19]

$$\eta_{II} = \frac{|\dot{W}_{rev}|}{|\dot{W}|} = \frac{|\dot{W}_{rev}|}{|\dot{W}_{rev}| + |\dot{W}_{loss}|}. \tag{2.7}$$

While a high Second-Law Efficiency does not always imply optimality of a process with respect to financial constraints, the DAC process which minimizes energy consumption, which indeed this publication focuses on, will also minimize irreversible losses, i.e., maximize second-law efficiency, as much as is economically feasible.

2.3 System-Level Analysis

2.3.1 Reversible Work for Separation

To begin, it is necessary to review the concept of thermodynamic reversible work requirements in the context of Direct Air Capture, particularly to illustrate the power-requirement implications of carbon dioxide's dilute atmospheric concentration.

Carbon Engineering's 1 Mt-CO_2/year plant is designed to remove 111.9 t-CO_2/h from the atmosphere, from a mass flow of 251,000 t-air/h with 0.060 mass-% CO_2 [1]. Given this data, their simulation was performed to correspond with an atmospheric CO_2 mole fraction of $X^i_{CO_2} = 0.000391 = 391$ ppm. While recent measurements give 416 ppm as of August 2021 [2], we will use 391 ppm to maintain conservative work estimates and to stay consistent with Carbon Engineering's data.

Figure 2.2 shows the relationship between the initial mole fraction X^i_α of a component α, i.e., CO_2, in an ideal gas stream and the minimum mole-specific work required for its isolation, considering no changes to total pressure and temperature. Two curves are plotted, one representing a final mole fraction of $X^f_\alpha = 0.90 X^i_\alpha$ in the gas stream (removal of 10% of the gas). The other was set to $X^f_\alpha = 0.257 X^i_\alpha$ (removal of 74.3% of the gas) to correspond with the Carbon Engineering plant's capture fraction.

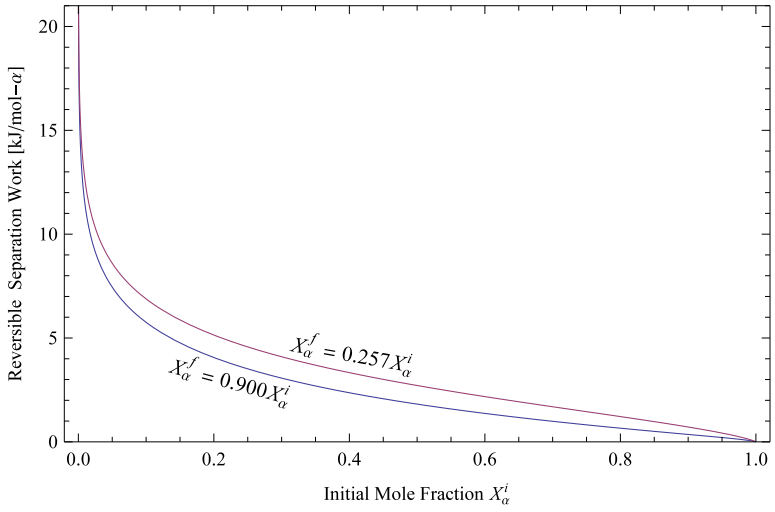

Figure 2.2: Reversible Mole-Specific Separation Work vs. Initial Gas Mole Fraction at T_0= 294 K

As can be seen in Figure 2.2, as the initial mole fraction of a component in a gas stream decreases, the minimum amount of mole-specific work required to separate it from the gas' other components increases exponentially. With temperature and pressure remaining constant, separation work is driven entirely by entropy of mixing.

For comparative purposes, with component α being CO_2 at 21°C, separation from flue gas in a coal-fired power plant with $X^i_{CO_2}$ = 0.15 [20] requires a minimum of 5.87 kJ/mol-CO_2 (133 MJ/t-CO_2)[1] to reduce its mole fraction by 74.3%. Separation from atmospheric air with $X^i_{CO_2} = 0.000391$, as in Carbon Engineering's case, requires a minimum of 20.48 kJ/mol-CO_2 (465 MJ/t-CO_2) to reduce its mole fraction by 74.3%, a ~3.5× increase.

At first glance, the factor of 3.5 may not appear to be a significant difference. However, considering the initial mole fractions in this comparison differ by three orders of magnitude, for every mole of CO_2 the DAC sorbent material is exposed to, 2557 moles of air must pass through the contactor. In contrast, only 6.67 moles of flue gas must pass through the power plant's sorbents to expose them to a mole of CO_2. Thus, while reversible separation work does not appear to be penalized significantly on a molar basis, the actual rates of work for DAC are implied to be much larger due to a 380× increase in the incoming gas stream's required molar flow rate – significant amounts of power (9.2 MW in Carbon Engineering's process [1]) must be dedicated simply to moving massive volumes of air through the sorbent material.

It should also be noted that while use of a weak base in the Air Contactor solution should theoretically result in lower energy demand for sorbent regeneration [21], a substantial increase in contactor area would be required as a consequence [22], and with it a proportional increase in fan power. Use of a strong base, as in Carbon Engineering's case, implies smaller contactor area compared to the weak-base approach, though a much higher quality of thermal energy for regeneration is required [22].

Caram et al. [21] introduce an approach to determine reversible work based on the energy required for this regeneration step. Our approach instead is to compare Carbon Engineering's plant to a general-

[1] In practice, point source capture has its own array of technical challenges, i.e., flue gas particulates and chemical sorbent contaminants. We consider it here only to illustrate the difference in minimum work required to capture from a dilute stream (DAC).

ized reversible DAC process based solely on entropy of mixing, i.e., the plot of Figure 2.2.

For Carbon Engineering's plant to remove 111.9 t-CO_2/h from its incoming air stream, we find a thermodynamic minimum power requirement of 14.46 MW for pure CO_2 leaving the plant at 21°C and 1 bar. Because the CO_2 is pressurized to 151 bar for pipeline transport and sequestration [1], we add the reversible work/power for isothermal compression (6.74 MW) to find the plant's total reversible work requirement as

$$\dot{W}_{rev}^{tot} = 21.20\,\text{MW}.$$

2.3.2 Reversible Natural Gas Use for CO_2 Separation

Still considering a reversible process, we ask for the amount of natural gas required for reversible CO_2 separation at 21°C. We estimate the natural gas mass flow rate by considering the mole-specific work potential of CH_4, which is, for combustion with pure O_2, simply its Gibbs Free Energy of Reaction,

$$\triangle \bar{g}_R(294\text{K}, 1\text{ atm}) = -800.8\,\text{kJ/mol}.$$

Here, we discount the additional work which may be obtained through reversible mixing of the combustion product stream [19]. Taking the quotient of the reversible work requirement (21.20 MW) and the mole-specific work potential gives a 1.53 t/h flow of CH_4, or 13.7 kg-CH_4/t-CO_2 separated for a 111.9 t-CO_2/h capture rate.

In practice, that is for the actual irreversible plant, a 19.7 t/h flow of CH_4 is required [1] (or 176.1 kg-CH_4/t-CO_2), corresponding to a work potential of 273.2 MW by the same calculation method.

Thus, for removal of 10 Gt-CO_2/year using a *fully reversible* process relying only on natural gas, an input of 13.7 Mt-CH_4/year (or ~2.06×10^{11} Nm^3/year) would be required. This would still be a substantial portion of yearly global production, corresponding to ~5.04% of 2019's production of 4.089×10^{12} Nm^3 [9].

With the actual process set to consume ~11.5 times more than this, one can expect that widespread deployment of DAC plants relying solely on natural gas as a feedstock would prove problematic from a resource-consumption perspective. In addition to this, the potential for fugitive methane emissions, both in upstream processing and within the plant, may hamper the plant design's negative-emissions credentials - indeed, the worst case would see a DAC plant which emits more CO_2-equivalent methane emissions than actual CO_2 it removes from the atmosphere.

2.3.3 Net Work Loss and Second-Law Efficiency

To estimate net work loss and second-law efficiency, we apply Eq. (2.4) over the entirety of the Carbon Engineering plant. Because all power is produced internally through use of natural gas as feedstock (no external work input, $\dot{W} = 0$), we find the net work loss as the total difference in $\dot{n}(\bar{h} - T_0\bar{s})$ terms in Eq. (2.4) for all flows entering and leaving the system. Figure 2.3 shows all inflows to and outflows from Carbon Engineering's plant, where the 'Air to ASU' and 'Depleted Air from ASU' streams were computed by mass and energy balances (Eqs. (2.1, 2.2) over the ASU, while the 'Turbine Combustion Air' stream assumed stoichiometric combustion to produce Carbon Engineering's reported NGCC outflows [1].

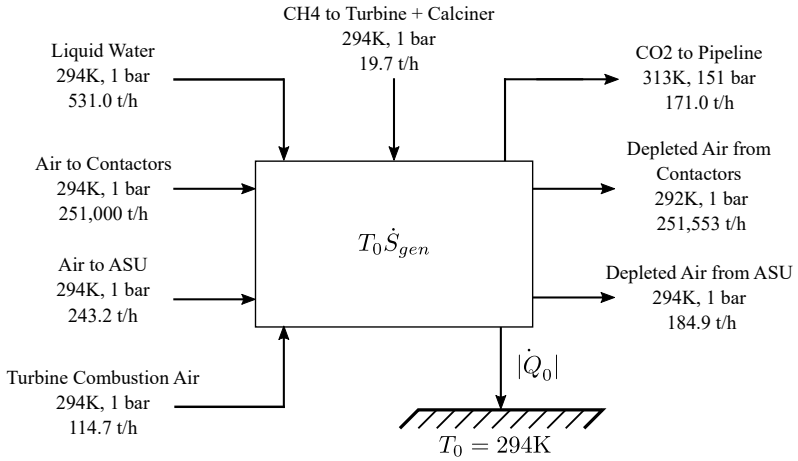

Figure 2.3: System-Level Flow Diagram of Carbon Engineering's baseline DAC Plant configuration

The 'CO2 to pipeline' stream is comprised of 97.12% CO_2, 1.36% O_2, 1.51% N_2 and 0.01% H_2O [1]. The natural gas configuration requires an Air Separation Unit (ASU) for fluidized bed combustion with pure O_2 in the Calciner, ensuring that combustion products consist primarily of CO_2 and water. We assume the ASU's air supply to contain an equal quantity of oxygen as is fed to the calciner (55.93 t/h), giving an incoming flow rate of 243.2 t/h for air containing 23% O_2 by mass.

Note also that while the Carbon Engineering plant diagram gives a 252,000 t/h mass flow leaving the air contactor [1], we use the non-rounded value of 251,553 t/h as obtained by mass balance with all other in/outflows of Figure 2.3.

For the system as shown in Figure 2.3, from Eqs. (2.4) and (2.5) we find the net work loss to entropy generation

$$\dot{W}^{tot}_{loss} = 258\,\text{MW}.$$

Together with the 21.20MW reversible work requirement, this yields

$$\dot{W}^{tot}_{loss} + |\dot{W}^{tot}_{rev}| = 279.2\,\text{MW}$$

as the overall work potential consumed by the system.[2]

We point out that while the system consumes 273.2 MW of work potential from natural gas (Section 2.3.2), the Air Contactor sees liquid water evaporating into the passing air which then leaves as vapor in the depleted air stream. This uncontrolled evaporation destroys ~4.2MW of work potential for the case of adiabatic evaporation (in which case the air-liquid mixture would leave at 16°C) to ~7.9MW for isothermal evaporation (the mixture leaving at 21°C). Taking the difference between the overall work potential consumed (279.2 MW) and the process fuel's work potential (273.2 MW), we estimate this additional loss to evaporation to be ~6 MW (or 2.3% of $\dot{W}^{tot}_{loss}$), which our calculation for $\dot{W}^{tot}_{loss}$ implicitly includes.

We do not consider this evaporative loss to be meaningful in the context of the process' evaluation, as the work being 'paid for' is the energy supply, with the exergy lost to evaporation being unharvestable

[2]The difference in compressor outflow temperatures, i.e., 21°C from the isothermal case versus 40°C in practice, correspond with <50 kW of difference in work loss values.

regardless. Thus, we also define the net loss quantity

$$\dot{W}_{loss}^{NG} = 258\,\text{MW} - 6\,\text{MW} = 252\,\text{MW},$$

which is the work lost from the work potential provided by natural gas. In this way the second-law efficiency, whose denominator should equal the actual work requirement in practice (Eq. (2.7)), is not penalized due to losses unassociated with the process' energy source.

Using $\dot{W}_{loss}^{NG} = 252\,\text{MW}$ in Eq. (2.7) with the plant's reversible work requirement (21.20 MW) gives the second-law efficiency

$$\eta_{II} = 0.078 = 7.8\%$$

for the natural gas 'A' configuration with CO_2 compression to 151 bar—this can be interpreted as the plant in practice consuming ~13× more energy than is theoretically required. This value agrees with other estimates for second-law efficiency of KOH-sorbent DAC processes, Sabatino et al. giving 7.6% - 7.9% [23].

Thus, opportunities are available to reduce power/heat consumption, and therefore cost per unit of CO_2 captured, through revision of the plant's internal processes – these will be explored and discussed in the component-level analysis section.

It should also be noted that heat exchange with the environment, that is, $|\dot{Q}_0|$, Figure 2.3, is strongly dependent on the temperature of the CO_2-depleted air leaving the Air Contactor, the temperature being below T_0=21°C due to evaporative cooling. For the given value of 19°C, $|\dot{Q}_0| = 75\,\text{MW}$, while for a 1°C increase to 20°C, $|\dot{Q}_0| = 0$. Work loss to entropy generation is affected by these changes to a much smaller degree, however, with the 1°C increase adding only an additional 0.4 MW of work loss.

2.4 Component-Level Analysis

In this section, we analyze the most energy-demanding components and subsystems within the plant and assess their contributions to the 252 MW work loss associated with natural gas use, looking in greater detail at the Calciner, Air Separation Unit, CO_2 Compression System and Power Island as shown in Figure 2.1. We will also look into the effects of chemical exergy dissipation throughout the plant, and tabulate all losses in Section 2.5.

2.4.1 Calciner and Preheat Cyclones

We begin by analyzing the calciner, the most energy-demanding component, with a total energy input of 186.91 MW, 99.6% of which is in the form of combustion heat [1].

The calciner's high thermal demand is largely unavoidable due to the high reaction enthalpy required for decomposition of calcium carbonate to calcium oxide and carbon dioxide ($CaCO_{3\,(s)}$–> $CaO_{(s)}$ + $CO_{2(g)}$, standard enthalpy of reaction $\triangle\bar{h}_R = 179\,\text{kJ/mol}$).

With no mixing entropies involved, as the decomposition yields only one gaseous species, the Law of Mass Action gives [19]

$$A = \sum_{\alpha} \gamma_\alpha \bar{g}_\alpha(T,p) = 0, \tag{2.8}$$

i.e., affinity A vanishes in chemical equilbrium. Here, $\bar{g}_\alpha(T,p) = \bar{h}_\alpha(T,p) - T\bar{s}_\alpha(T,p)$ is species α's Gibbs Free Energy. γ_α is the same species' stoichiometric coefficient, being negative in sign if consumed

by the reaction, and positive if produced.

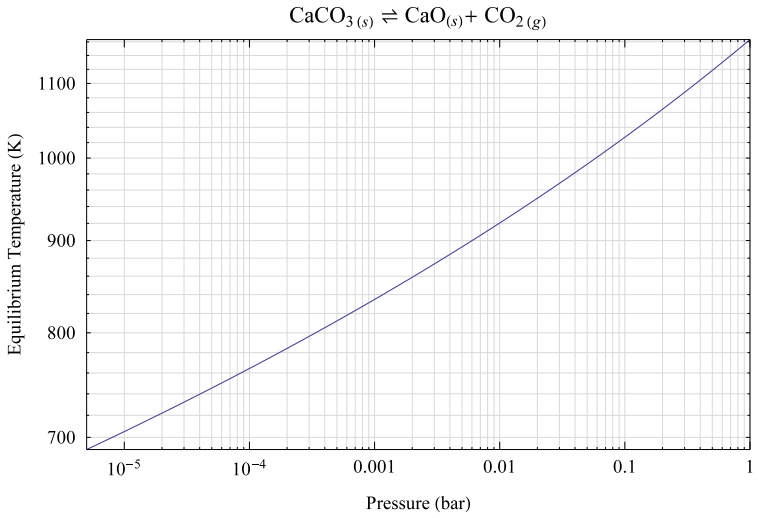

Figure 2.4: $CaCO_3$ Decomposition Reaction Equilibrium Temperature versus Pressure, Logarithmic Plot

The reaction's equilibrium temperature as a function of pressure, obtained as the solution of Eq. (2.8), is shown in Figure 2.4. For the existing design with calciner operation at an internal pressure of 1 bar, the equilibrium temperature is 1163 K (890°C), reducing by 45 K to 1118 K (845°C) with a 50% reduction of internal pressure, and more substantially by ∼136 K to 1027 K (754°C) for a 90% pressure reduction.

Overall, the calciner's required equilibrium temperature decreases as calciner pressure is reduced, though substantial decreases in temperature are only seen as internal pressure approaches a vacuum (Figure 2.4). The question therefore remains as to how pressure reduction to near-rarefied conditions may be accomplished in practice. One can speculate that the work required by pumps to maintain a vacuum would likely exceed any energy saved through marginally reducing the calciner's operating temperature, while the complexities of sealing such a system against atmospheric pressure would certainly increase technical risk and overall costs. Thus, operation outside of ambient pressure can safely be assumed to be a costly and impractical solution to reduce energy demand.

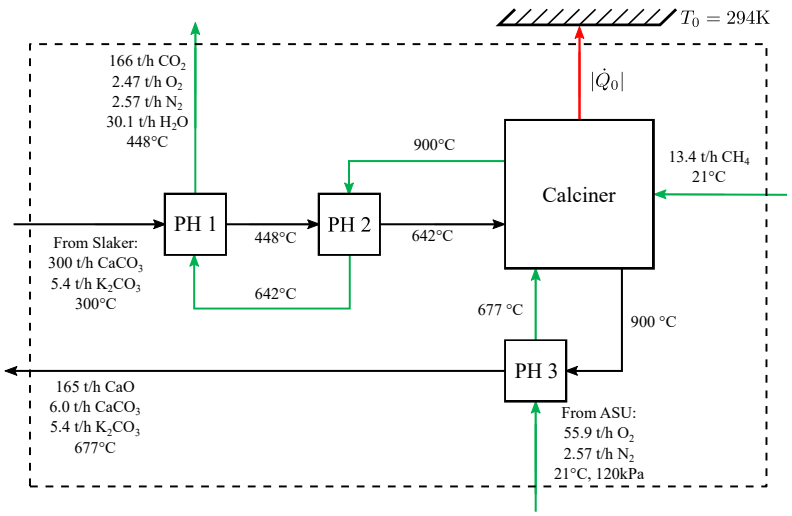

Figure 2.5: Calciner and Preheat System for Natural Gas Configuration

Figure 2.5 shows the calciner and preheater system as adapted from Carbon Engineering's data, with flows of gases shown in green and solids in black – this is represented simply by the 'Calciner' block in Figure 2.1. All flows enter and leave the system at atmospheric pressure, with the exception of the oxygen stream from the Air Separation Unit which is provided at 120 kPa. Due to lack of data available for the preheat cyclones (PH1, PH2 and PH3), they were treated as adiabatic with perfect heat exchange between flows, i.e., all flows exiting at the same temperature. For consistency with Carbon Engineering's simulation data, we omit the small flow of filtered $CaCO_3$ fines from the pellet reactor as an incoming flow to the first preheater [1]. With these assumptions, the resulting temperatures found, as labelled in Figure 2.5, were reasonably close to those obtained by Carbon Engineering in their simulation, the largest discrepancy being 642°C as the highest possible temperature at which flows may leave the second preheater. For this value, Carbon Engineering reports 650°C [1].

Applying the energy balance to the system shown, we find a net heat loss $|\dot{Q}_0| = 6.6\,\text{MW}$ to the environment at 21°C. Through the entropy balance Eq. (2.4), we find

$$\dot{W}^{calc}_{loss} = 63\,\text{MW} \;\; (25.0\%\text{ of } \dot{W}^{NG}_{loss}),$$

that is 63 MW of destroyed work potential due to irreversible chemical reaction, i.e., chemical exergy dissipation, and heat transfer between gaseous and solid material flows. Further discussion on calciner heat transfer as it relates to thermal demand and work loss is available in Sec. 3.1.

To estimate the thermal efficiency of the calciner, we compare existing data to an idealized system in which reactant ($CaCO_3$) and product (CaO and CO_2) enter and leave at 300°C, respectively, and react at 900°C. We find this simplified system to require 145 MW of heat, of which 136 MW is used to sustain the $CaCO_3$ decomposition reaction, the remainder being the net amount consumed in pre-heating and cooling the pellet stream. Using this 145 MW as a baseline to compare its actual 186.11 MW thermal demand, we find the calciner to be 78% thermally efficient, consistent with Carbon Engineering's value [1].

2.4.2 Air Separation Unit

The ASU produces a flow of 58.5 t/h of gas mixture, primarily oxygen (95.60% by mass), and requires 13.3 MW of power [1], corresponding to ∼58% of the plant's reversible work requirement. Applying the principles of Section 2.3.1, where we assume waste gas from air purification (N_2, CO_2 and H_2O) leaves at the same temperature and pressure at which it originally enters, we find the reversible work requirement for the ASU to be $|\dot{W}_{rev}| = 2.9$ MW. This value corresponds with a pressurized product stream at 120 kPa [1], giving a second-law efficiency of 21.8% for the ASU. For an unpressurized product stream, we find only a small difference, where $|\dot{W}_{rev}| = 2.7$ MW. Due to the inherent difficulty of air separation, requiring large temperature and pressure swings for liquefaction and fractional distillation, the air separation unit contributes a substantial irreversible work loss of

$$\dot{W}_{loss}^{ASU} = 10.4\,\text{MW} \;\; (4.1\% \text{ of } \dot{W}_{loss}^{NG}).$$

2.4.3 Water Knockout

After leaving the preheat cyclones (Figure 2.5), the hot calciner off-gas stream is used to superheat steam for power production as shown in Figure 2.6. Using data from Carbon Engineering's simulation, we find it to deliver 9 MW of heat to the superheater for an incoming temperature of 454°C and an outgoing temperature of 325°C [1]; using our own value of 448°C as the incoming temperature, we obtain an exit temperature of 319°C by energy balance for the same superheater heating rate. The cooled gas then passes through a knockout drum where it is sprayed with incoming water to condense and remove a portion of its moisture before delivery to the intercooled compression system, while liquid water is diverted to wash $CaCO_3$ pellets before their arrival in the slaker [1].

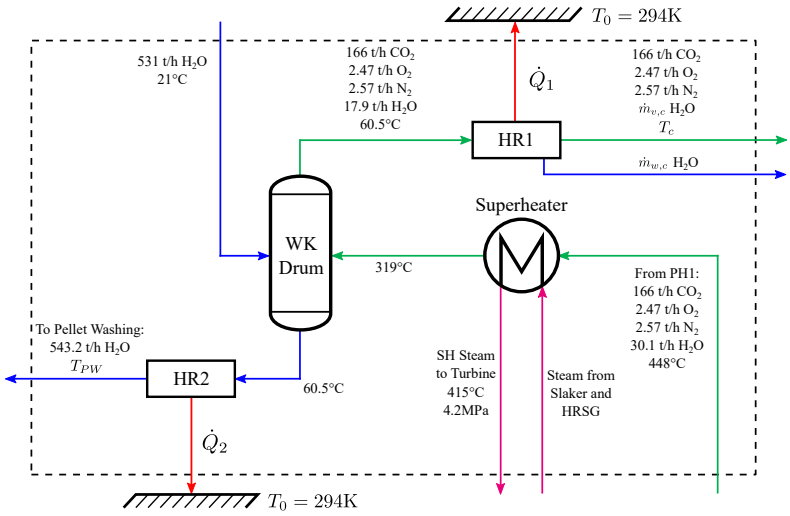

Figure 2.6: Superheater and Water Knockout Drum for Natural Gas Configuration

Figure 2.6 shows a general schematic of the water knockout system. For analysis purposes, we treat the knockout drum as adiabatic with two heat removal steps added: one for the gas stream to the compression system, and the other for liquid water to the pellet washer (labelled HR1 and HR2, respectively in Figure 2.6). HR1 can serve to represent the cooling stage prior to the first compression stage, as is typical to minimize compression work via temperature and gas volume reduction [24], where

additional water is condensed and removed, presumeably being diverted to the pellet washing station. This flow of condensed water is labelled $\dot{m}_{w,c}$, where its value and those of variables $\dot{m}_{v,c}$ (mass flow of vapor to the 1st compressor inlet) and T_c (flow temperature at 1st compressor inlet) depend on heat removal rate $\dot{Q}_1$.

Though it is unclear from Carbon Engineering's paper [1] whether a specific water temperature is necessary for pellet washing, $\dot{Q}_2$ represents the heat removal rate associated with cooling the liquid water stream leaving the drum to T_{PW}, the temperature at which water arrives at the washing station. Thus, the total heat removed from the system is calculated simply as $\dot{Q}_r = \dot{Q}_1 + \dot{Q}_2$.

We model all components to operate at ambient pressure (1 bar) with the incoming water stream at ambient temperature (21°C). For simplicity, we ignore dissolution of carbon dioxide, oxygen or nitrogen in water. As a result, we find the knockout drum's internal temperature to be 60.5°C, where 17.9 t/h of water leaves as saturated vapor with the gas stream, and 543.2 t/h leaves as liquid to the pellet washing station.

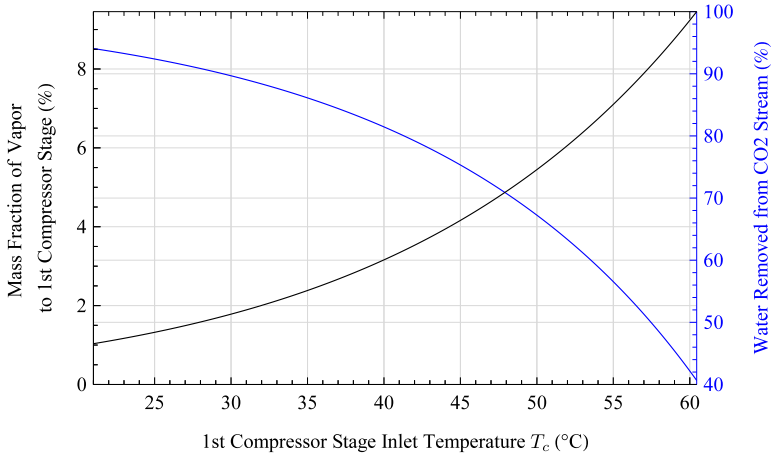

(a) Vapor Mass Fraction and Water Removal Fraction

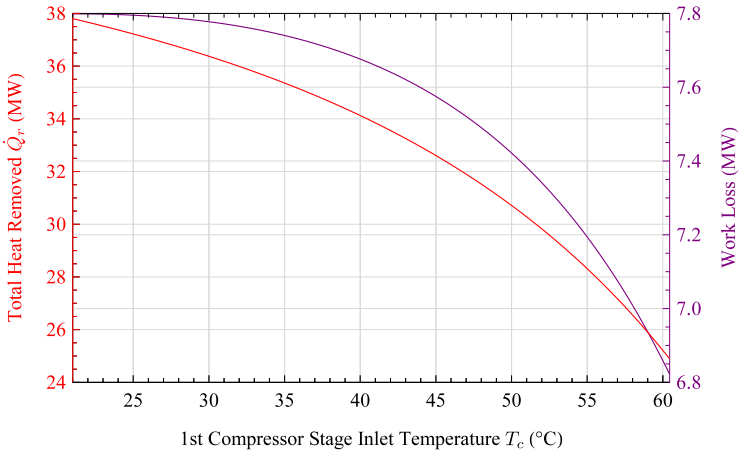

(b) Heat Removal Rate and Work Loss

Figure 2.7: Vapor Mass Fraction, Water Removal Fraction, Heat Removal Rate and Work Loss as functions of Flow Temperature at 1st Compressor Inlet ($T_{PW} = 21°C$)

The plots of Figures 2.7(a) and 2.7(b) visualize how heat removal rate, work loss, vapor mass fraction and water removal fraction relate to the temperature at the inlet of the 1st compressor stage (T_c). To produce the plots, we fix the washing station water temperature at $T_{PW} = 21°$C, where we find $\dot{Q}_2 =$ 24.9MW. Water removed (%) is calculated as the percentage change in water content of the knockout drum's incoming and outgoing gas flow.

Figure 2.7(a) shows that lower temperatures of the gas flow to the 1st compressor inlet correspond with lower water vapor content, while Figure 2.7(b) shows that in order to realize these lower temperatures, increasing amounts of cooling power are required. Therefore, if additional compression work due to vapor content is to be avoided, adequate cooling of the gas stream leaving the knockout drum is a necessity.

We find the superheater/knockout drum system's maximum work loss to be

$$\dot{W}_{loss}^{WK} = 7.8\,\text{MW} \;\; (3.1\% \text{ of } \dot{W}_{loss}^{NG}),$$

equal in value to the maximum available work associated with bringing the superheater's outgoing stream from 319°C to the temperature of the surrounding environment (21°C). It should be noted that lower values of work loss in Figure 2.7(b) do not necessarily imply improvement to the second-law efficiency of the plant as a whole - they simply reflect differences in thermomechanical work potential between the water knockout system's incoming and outgoing flows. Because lower work loss in the knockout system implies higher outgoing temperature T_c and vapor content for the CO_2 stream, the intercooled compression system's power and cooling requirements would increase as a result [24]. Thus, improvements to the water knockout system would recover up to 7.8 MW of work or 37.8 MW of medium-grade process heat from the 319°C CO_2 stream prior to its arrival in the knockout drum, thereby minimizing heat removal requirements for optimal compressor inlet conditions. For all flows exiting the system (Figure 2.6) at 21°C, we find an additional 12.9 MW of heat removal to be required prior to the first compressor stage to minimize the CO_2 stream's water vapor content to 1.03%.

2.4.4 CO_2 Compression System

As aforementioned, the reversible work requirement for isothermal compression of a pure CO_2 stream (111.9 t/h) was found to be 6.74 MW for a delivery pressure of 151 bar. Accounting for additional CO_2 from natural gas combustion in the Calciner and Gas Turbine (54.1 t/h for a total 166 t/h output CO_2 stream, Figure 2.6), the isothermal reversible work requirement becomes ∼10.0 MW.

Use of an idealized four-stage compression unit with intercooling, where pure CO_2 is cooled to $T_0 = 21°C$ after each isentropic, adiabatic compression stage, we find the minimum reversible work requirement to be 12.2 MW, i.e., an additional 2.2 MW being required compared to the isothermal case, where we used the pressure ratios 4.43, 3.96, 3.30 and 2.57, respectively for each compression stage. These pressure ratios were obtained using Particle Swarm Optimization to minimize total reversible work as a function of intermediate pressures p_1, p_2 and p_3, where initial pressure $p_0 = 101.325$ kPa and final pressure $p_4 = 15100$ kPa were fixed, and no intercooling pressure drop was assumed. Properties were calculated based on Span and Wagner's Equation of State for CO_2 [18].

Note that here, we did not include the influence of O_2, N_2, and H_2O due to difficulty in predicting the quaternary mixture's thermodynamic behavior outside of the ideal gas region. The author of Ref. [25] considers multi-stage compression of a CO_2/saturated vapor mixture. Using the same data in our

calculations as in Ref. [25], we find a <1.6% difference in final work estimates. Thus, we deemed our work estimate reasonable owing to CO_2's large mass fraction (>97%).

It should also be noted that in this case, with CO_2 transitioning to the liquid phase at 21°C, 58.66 bar, the fourth compressor would act as a pump for a portion of the process. In practice, it may be necessary to ensure CO_2 maintains a vaporous or supercritical state to avoid equipment complications.

Carbon Engineering gives a 22 MW power requirement for their compression system [1]. Thus, the 12.2 MW reversible work value gives an irreversible loss of

$$\dot{W}_{loss}^{comp} = 9.8\,\text{MW} \;\; (3.9\% \text{ of } \dot{W}_{loss}^{NG}).$$

It should be noted that a significant portion of compression work is dedicated to processing CO_2 from natural gas combustion. Using Carbon Engineering's compressor power estimate of 132 kWh/t-CO_2 [1], the 54.1 t-CO_2/h produced by gas combustion between the NGCC power island and calciner corresponds to an additional 7.1 MW of compressor power demand (or 32% of its total 22 MW power demand). This value becomes 4.0 MW for reversible four-stage compression, or 3.3 MW for isothermal compression.

Indeed, the handling of CO_2 produced by natural gas is critical for the plant to maintain its net-negative credentials, though it lends credence to the argument that use of hydrocarbon fuels for a carbon-removal installation is counterproductive. In the context of energy use, it is clear that energy savings may be realized through eliminating use of natural gas, primarily in the calciner in which it plays its most dominant role. Additionally, integration of intercooling stages with a preheat system for steam cycle feedwater (namely, for the Slaker and Steam turbine system) may be a productive route to explore. This concept and its potential for energy savings is discussed in detail by Romeo et. al. [24].

2.4.5 Power Island

In the plant's 'A' configuration, a combined cycle gas turbine (CCGT) power plant is used to produce power for all components, where a GE LM2500 DLE combined cycle 2×1 system is used [1][26]. While in practice, the system's steam turbine will consume steam from both the slaker and the CCGT system's heat recovery steam generator, Carbon Engineering models steam cycles for the slaker (9.8 MW of power produced) and the CCGT system (46 MW of power produced) independently for simplicity [1]. Using this modelling procedure, determination of irreversible losses is also made relatively simple.

The CCGT power plant's loss to irreversibilities is easily determined by considering the work potential of its fuel. Using the reported rate of CH_4 consumption, that is 6.3 t/h [1], with the Gibbs Free Energy of Reaction $\triangle \bar{g}_R(294\text{K}, 1\text{ atm}) = -800.8\,\text{kJ/mol}$ (Section 2.3.2), the fuel's work potential is determined to be 87.5 MW, i.e., the CCGT system sees a loss of

$$\dot{W}_{loss}^{CCGT} = 41.5\,\text{MW} \;\; (16.4\% \text{ of } \dot{W}_{loss}^{NG})$$

to irreversibilities given its 46 MW net power production. Note that the fuel's work potential may also be found by dividing the produced 46 MW by General Electric's published efficiency value (52.9%) for the 60Hz, 2x1 configuration in question [26].

Using the mass flow and state of post-superheat slaker steam provided by Carbon Engineering (70.2 t/h at 415°C, 4.2 MPa) in combination with their condenser's operating temperature of 50°C [1], we find a fully-reversible, adiabatic (i.e., isentropic) turbine would produce 20.8 MW of power with a vapor quality of 83% at its exit. Thus, with 9.8 MW of reported power production, the steam turbine

contributes an irreversible loss of

$$\dot{W}_{loss}^{ST} = 11\,\text{MW} \;\; (4.4\%\text{ of } \dot{W}_{loss}^{NG}).$$

2.4.6 Chemical Exergy Dissipation (External to Calciner) and Other Losses

The keen observer will notice that while natural gas provides 186 MW of work potential to the calciner, only 63 MW of this potential is destroyed within its system boundaries (Section 2.4.1). Hence, ∼123 MW of work potential leave the calciner with the outgoing flows, where ∼24 MW leave as thermomechanical exergy to the steam superheater (CO_2, O_2, N_2, H_2O at 448°C, ∼13.5 MW) and slaker (CaO at 677°C, ∼10.8 MW).

The remaining 99 MW provided by natural gas are stored as chemical exergy, which in fact is almost entirely attributable to the Gibbs Free Energy of Reaction for $CaCO_3$ decomposition at $T_{0,}$

$$CaCO_3 - > CO_{2(g)} + CaO\text{: } \triangle \bar{g}_R(294\,\text{K}, 1\,\text{bar}) = 131.9\,\text{kJ/mol},$$

with 294 t/h of $CaCO_3$ undergoing reaction.

This exergy, in principle, could be converted to useful work downstream, though this is not done in the process as presented. Instead, further downstream, the vast majority of this chemical exergy is released as heat of reaction [1] in the slaker, pellet reactor and air contactor, with respective chemical reactions

$$CaO + H_2O \text{ -> } Ca(OH)_2\text{: } \triangle \bar{h}_R = -63.9\,\text{kJ/mol},$$

$$K_2CO_3 + Ca(OH)_2 \text{ -> } 2KOH + CaCO_3\text{: } \triangle \bar{h}_R = -5.8\,\text{kJ/mol},$$

$$CO_{2(g)} + 2KOH_{(aq)} \text{ -> } H_2O_{(l)} + K_2CO_{3(aq)}\text{: } \triangle \bar{h}_R = -95.8\,\text{kJ/mol}.$$

Due to relatively small heat of reaction, the loss in the pellet reactor is of less importance, where 5.7 MW of heat are released for a 0.979 kmol/s $Ca(OH)_2$ flow in solution. A portion of the heat released in the slaker, which is 52.2 MW for a 165 t/h CaO flow, contributes to steam generation for the turbine, recovering 9.8 MW of work potential, and as process heat for feedwater (see the Lime Cooler [1]).

The exothermic reaction in the Air Contactor releases 67.7MW of heat for 111.9 t/h CO_2 captured. However, because air and KOH solution flow through the Air Contactor in such massive volumes, the reaction heat released imparts a negligible temperature change in them. We note that while the air passing over the sorbent material is indeed cooled by evaporative cooling from the KOH solution, due to the reaction heat released, the cooling effect is slightly reduced. Overall, because the stored chemical exergy of natural gas is freed here at low temperature, no work recovery is possible, as can be seen in the second term of Eq. (2.4).

Thus, one may argue that losses from the calciner far exceed the 63 MW which we determine for the process within the boundaries of the calciner system (Figure 2.5). Indeed, the large (endothermic) heat of reaction demanded for decomposition of $CaCO_3$ not only leads to the calciner's high temperature requirement (>890°C, Section 2.4.1) and corresponding losses in heat transfer, but also to a large amount of stored chemical exergy in CaO which can then only be partly recovered, it being largely dissipated as low-grade heat into the environment via the Air Contactor. Therefore, the excessive energy required to

recover CO_2 from $CaCO_3$ may be argued to be the chief driving factor behind large irreversible losses in Carbon Engineering's plant.

We note that the large amount of air which must be moved through the air contactor requires a significant amount of power (9.2 MW [1]) to drive the fans. Based on our formulation of the system (2.3), i.e., with respect to thermodynamic separation work (Section 2.3.1), we consider this to be a total loss (3.7% of $\dot{W}_{loss}^{NG}$).

While we do not analyze the chemical mechanisms for chemical exergy dissipation in the slaker, pellet reactor, and air contactor in detail, when considering the net work loss with respect to energy consumed $\dot{W}_{loss}^{NG} = 252\,\text{MW}$, with 152.7 MW accounted for, the remaining loss of work potential to irreversibilities becomes

$$\dot{W}_{loss}^{chem+other} = 99.3\,\text{MW} \;\; (39.4\% \text{ of } \dot{W}_{loss}^{NG}).$$

2.5 Summary of Major Losses

Carbon Engineering's proposed DAC plant removes 111.9 t-CO2/hr from ambient air while consuming 273.2 MW of work potential from natural gas. As aforementioned, the thermodynamically required minimum, i.e., reversible, work for separation and compression for this process is $\dot{W}_{rev}^{tot} = 21.20\,\text{MW}$. Hence, a total loss of $\dot{W}_{loss}^{NG} = 252\,\text{MW}$ occurs due to irreversibilities in the various subprocesses of the DAC system, or a loss of $\dot{W}_{loss}^{tot} = 258\,\text{MW}$ when accounting for evaporation of water in the air contactor (see Section 2.3.3). Table 2.1 summarizes these losses as described in Section 2.4.

Source of Loss	**Irrev. Loss $\dot{W}_{loss}$ (MW)**	**% of $\dot{W}_{loss}^{tot}$**	**% of $\dot{W}_{loss}^{NG}$**
Chemical Exergy Dissipation (Ext. to Calciner) + Other	99.3	38.5%	39.4%
Calciner	63.0	24.4%	25.0%
Combined-Cycle Gas Turbine	41.5	16.1%	16.4%
Steam Turbine	11.0	4.3%	4.4%
Air Separation Unit	10.4	4.0%	4.1%
Compression System	9.8	3.8%	3.9%
Air Contactor Fans	9.2	3.6%	3.7%
Water Knockout	7.8	3.0%	3.1%
Air Contactor Evaporation	6	2.3%	-
Total:	**258**	**100%**	**100%**

Table 2.1: Major losses to irreversibilities in Carbon Engineering's 1 Mt-CO_2/yr plant as percentages of total thermodynamic loss, and of total loss less water evaporation

2.6 Discussion

We accounted for 152.7 MW of irreversible losses by detailed analysis of individual components, viz. the calciner, CCGT system, steam turbine, ASU, compression system and water knockout, with the contactor fans' power requirement (9.2 MW) being considered a total loss. The remaining 99.3 MW of losses are owed to the combined effects of uncontrolled chemical reactions and thermal dissipation in the air contactor, pellet reactor and slaker.

In the 'A-configuration' studied, all energy, and hence exergy, supply is through natural gas, with 186 MW fed directly to the calciner and 87 MW fed to the Power Island. With 92.4% of incoming exergy lost to irreversibilities, we can state that the largest irreversible losses are attributable to exergy dissipation in exothermic chemical reactions, the second-largest occurring within the calciner itself. Based on our analysis, we find an overall second-law efficiency of 7.8% for Carbon Engineering's plant based on a minimum (reversible) work requirement of 21.20 MW.

2.6.1 Natural Gas Use in the Calciner

The 186 MW of energy entering the calciner, provided via natural gas, is mostly used to drive the endothermic calcium carbonate reaction ($CaCO_{3\,(s)} \rightarrow CaO_{(s)} + CO_{2(g)}$). However, some is consumed in heating incoming solids and combustion products (CO_2, H_2O) to the calciner's operating temperature (1173 K), as is required for reaction equilibrium (Section 2.4.1). The calculated 63 MW work loss in the calciner is mainly due to devaluation of the natural gas—which has a work potential close to its heat of reaction [19]—by combustion into a very hot product and subsequent heat transfer into the hot solid (CaO) outflow, where irreversible mixing of flows and entropy generation through the uncontrolled chemical reaction are also significant contributors.

In addition to the largely unavoidable irreversible losses associated with its use as a calciner feedstock, the use of natural gas as an energy source for liquid-sorbent DAC processes bears further discussion for a variety of reasons:

- Natural gas is non-renewable, hence a resource of finite supply must be exploited for a relatively inefficient process. If natural gas is to be involved as an energy source for DAC, its usage should be restricted only to those applications which cannot be powered by other means.
- For each ton of CO_2 removed from air, the use of natural gas adds ~½ ton of CO_2 from combustion. This not only increases the compressors' power requirements by ∼50% (Section 2.4.4), but also necessitates ∼50% larger cavities (or 50% larger volumes of reactive rock [27]) for long-term CO_2 storage. If the use of DAC increases into the future, so will the value of suitable space for permanent storage, space which should not be unnecessarily occupied by CO_2 produced within the capture process itself.
- As mentioned in Section 2.1, if DAC is to be implemented on a meaningful scale with respect to IPCC removal rate targets [4], exclusive use of natural gas-driven processes such as Carbon Engineering's 'A' configuration with its determined second-law efficiency will require over half of the world's current natural gas production [9], likely increasing the price of the commodity unless its production increases proportionally.
- One could argue, however, that if natural gas is to be used substantially in the future, it should be used in processes such as DAC which allow for capture and storage of the resulting CO_2, though its use for power generation with Carbon Capture and Storage may be more productive.

While the more minor losses between the water knockout and compression systems may be partially avoided if natural gas use is curbed, we also note that if natural gas use persists, the water knockout system in particular presents the opportunity to recover up to 37.8 MW of medium-grade process heat from the gas stream leaving the superheater, equivalent to 7.8 MW in work potential. A simple steam cycle may harness at least some of this potential to power smaller components or auxiliary systems (requiring 2.6 MW in total [1]).

2.6.2 Renewable Energy Use

For sustainable operation of DAC processes, the use of renewable energy sources as substitutes for natural gas must be considered. While we leave the proposal and detailed analysis of alternative configurations to the future, we briefly estimate the possible impacts:

The power required to drive the Carbon Engineering process is partly obtained through heat recovery from exothermic chemical reactions, though most power is derived from combustion of natural gas in the gas turbine(s). Replacing natural gas use with renewable energy sources, such as wind, solar, etc. will require, at minimum, some modifications to the system's management of process heat.

Use of renewable energy for the calciner may be possible, two options being through direct electrical heating, or replacing natural gas with green hydrogen (i.e., electrolysis of water using electricity provided from renewable sources), barring considerations for land use, energy storage to accompany the method of renewable power production, and other technical risks. Likewise, the NGCC power island may also be replaced provided enough renewable capacity is installed – doing so would avoid 17.3 t-CO_2/h from combustion being introduced to the plant for processing, reducing necessary $CaCO_3$ production by 39 t/h.

With an electrolyser splitting water into stoichiometric amounts of fuel (H_2) and oxidizer (O_2), and with electrical heating requiring no combustion, both modifications would eliminate the need to provide an oxygen stream for oxy-fuel combustion in the calciner. Hence, in both scenarios, the ASU is removed, reducing the power requirement by 13.3 MW. At the same time, the additional 54.1 t-CO_2/h produced from natural gas combustion in the calciner and NGCC unit is eliminated from the calciner's product stream, reducing the compression system's power requirement by ~7.1 MW (~32%, Section 2.4.4).

By these estimates, use of renewable energy for power and calciner heat would reduce the plant's mechanical power demand (between the ASU and Compressors) by ~20.4 MW.

2.6.3 Green Hydrogen Configuration

Assuming green hydrogen to be used in the calciner and the NGCC system to be replaced with renewable power, processing 111.9 t/hr of CO_2 captured from the atmosphere would require a ~261 t/h flow of $CaCO_3$, reducing the calciner's thermal energy requirement to ~162 MW (estimated at 3.18 GJ/t-CaO with 78% thermal efficiency, assuming 6.0 t-$CaCO_3$/h is rejected back to the pellet reactor [1]). Use of hydrogen combustion ($2H_2$ + O_2 -> $2H_2O$: $\triangle \bar{h}_R = -241.8$ kJ/mol) to meet this demand would require a feed of 4.86 t/h H_2, or 53,892 Nm^3-H_2/h, and 38.5 t/h O_2 (both produced via electrolysis). Likewise, the gas flow leaving would consist of 43.3 t/h H_2O and 111.9 t/h CO_2, a total flow of ~155 t/h as opposed to 201 t/h from the natural gas configuration (Figure 2.5).

For a commercially-available electrolyzer, we select ThyssenKrupp's Advanced Alkaline Water Electrolyzer modules, their '20 MW' module producing 4000 Nm^3-H_2/h with a DC power consumption of 4.3 kWh/Nm^3, and their '10 MW' module producing 2000 Nm^3-H_2/h for the same DC power consumption [28]. To produce the 53,892 Nm^3/h demanded by the new calciner, thirteen '20 MW' units and one

'10 MW' unit may be used, resulting in ~232 MW of DC power required for the electrolyzer stack, along with an added flow of 54 t/h of water. Additional water knockout capacity would also be required to accommodate the added 13.2 t/h of water produced as a combustion product.

Finally, assuming all other plant components to demand the same amount of power as in the 'A' configuration [1], and accounting for the compressors' reduced power requirements and elimination of the ASU and NGCC CO_2 absorber, an additional 35 MW of renewable power would be required to replace the previous NGCC power island.

Thus, by these very simplified estimates, use of a green hydrogen-fired calciner and a renewable power island would reduce overall energy demand to roughly 232 MW + 35 MW = 267 MW of renewable electrical energy, assuming no inverter losses for the power island. This corresponds to a 2.2% decrease compared to the natural gas configuration demanding 273.2 MW, where a portion of work losses would now be owed to the inefficiencies of electrical-to-chemical energy conversion in the electrolyzer. The question therefore remains whether any benefits of this configuration, namely, reduced CO_2storage space requirements, are worth its costs, i.e., the purchase and maintenance of large electrolyzer stacks, and installation of enough renewable capacity to reliably provide 267 MW of power with the necessary electrical and hydrogen storage.

We leave to future work a detailed comparison to the natural gas configuration which, during a period of global energy system transition, may be the better choice.

2.6.4 All-Electric Configuration

With the calciner being directly heated via electricity, and with the power island being replaced with only renewable capacity as discussed above, there would be no combustion products, and hence no losses to mixing of gas flows nor additional heat/power requirements for these products' processing (see Section 2.4.3). With the same reduction of 20.4 MW for the ASU and compression system, and again considering the calciner's thermal demand to be 162 MW with the remaining power demand totalling 35 MW, we estimate the plant's net energy consumption to be 162 MW + 35 MW = 197 MW, where all electrical power input to the calciner is released as heat.

Thus, on the basis of energy consumption, an all-electric plant configuration would likely be the ideal option to pursue. However, use of electric heating for the calciner begs the question of how $CaCO_3$ pellets are to be fluidized, possibly using a flow of recirculating CO_2, and the energy inputs required for this fluidization system.[3].

Regardless of how heat is provided, though, a minimum of $q_{calc}^{min} = 1.66 \frac{\text{GJ}}{\text{t-CaCO}_3}$ will always be required to sustain $CaCO_3$'s decomposition given its enthalpy of reaction

$$\triangle \bar{h}_R(900^\circ\text{C}, 1\text{ bar}) = 166.2\,\text{kJ/mol},$$

or $\dot{Q}_{calc}^{min} = 117\,\text{MW}$ for a 261 t/h flow of $CaCO_3$ with 6 t/h not consumed. Given this minimum amount of heat, for electrical heating we estimate the minimum entropy generation as [19]

$$\dot{S}_{gen} = \frac{\dot{Q}_{calc}^{min}}{T_H} = \frac{\dot{W}_{elec}^{min}}{T_H},$$

hence the minimum work loss

[3] See Section 3.2.

$$\dot{W}_{loss}^{min} = T_0 \dot{S}_{gen} = \frac{T_0}{T_H} \dot{W}_{elec}^{min} = 29.3\,\text{MW},$$

where T_H = 1173 K is the Calciner's operating temperature. [4]

We also note that an all-electric plant configuration may be difficult to realize in practice, primarily owing to the difficulty of efficiently providing process heat at 900°C to the Calciner. The massive installed capacity of intermittent renewables such as solar and wind must also be taken into account.

For the full plant, including an electric calciner, to be powered by renewables, McQueen et al. [29] estimate requirements of between 750 MW to 1100 MW of installed solar capacity with 4400 MWh to 5100 MWh of battery storage, or 500 MW of installed wind capacity with 3200 MWh of battery storage, both of which have significant cost implications. By their estimates, nuclear and geothermal power tie for the lowest installed capacity of 240 MW (given nine DAC plants being powered by a 2200 MW nuclear facility [29]). Logically, these requirements would be even larger for the hydrogen configuration discussed earlier.

It will also be necessary to examine improvements or pitfalls which may be realized downstream of the Calciner through eliminating natural gas use, particularly with regard to internal power generation from heat released throughout the system (i.e., decreasing the degree of steam superheat due to the Calciner products' reduced mass flow and/or heat capacity, Figure 2.6).

2.6.5 Losses of Chemical Exergy, External to the Calciner

In the natural gas configuration, the material leaving the calciner carries ∼124 MW of chemical and thermomechanical exergy. As discussed earlier, the chemical exergy is released in the exothermic reactions in Slaker, Pellet Reactor, and Air Contactor. In the latter, 67.7 MW of heat of reaction are dissipated into the passing air, which independent of the primary energy source remains irretrievable.

While quantities of heat released by each chemical reaction are easily determined, accurate accounting of un-harvested chemical and thermomechanical exergy was not performed as part of this analysis. Thus, future work must analyze the slaker, pellet reactor and air contactor components in detail to paint a clearer picture of the dissipation of exergy downstream of the calciner, i.e., the extent to which it is used for CO_2 separation, recovered as work, or irretrievably lost to the environment. Once these studies are performed, process improvements may be proposed which would ideally further reduce the plant's energy consumption in a cost-effective manner.

2.7 Summary, Outlook and Opportunities for Future Work

Carbon Engineering's DAC system as presented in Ref. [1] relies on natural gas as an energy source, and requires ~13 times the thermodynamic minimum energy supply. In other words, only ~8% of energy supply is used for the actual task of separating CO_2 from air, while the remaining 92% is consumed by irreversible processes throughout the system. Our thermodynamic analysis aims to give insight into the major locations and causes of these losses, which we regard as an important step for development of improved alternative processes.

The most significant losses are attributed to the chemical steps within the system, where high temperature and large heat of reaction in the endothermic calciner reaction, coupled with the impossibility

[4] More detailed estimates for power demand and work loss are presented in Chapters 3 and 4.

of energy recovery in the Air Contactor's exothermic reaction, result in unavoidably high energy demand. Reduction of the associated losses appears to be impossible for the present reactions, which, however, are feasible, and work well. Alternative chemical cycles may reduce these losses.

Our simplified estimates show that the use of renewable energy with an electrically heated calciner may reduce the energy requirements of Carbon Engineering's DAC process, where we estimate a 20.4 MW reduction in power requirements due to elimination of the ASU and a smaller mass flow being processed by the compression system, and a 24 MW reduction in the calciner's thermal demand due to a reduced $CaCO_3$ input. These benefits, however, may be outweighed by the financial costs of installing and maintaining the required renewable capacity [29].

With a single, all-electric plant consuming a minimum of 197 MW to remove 111.9 t-CO_2/h at high capacity factor (>0.90), removal of 10 Gt-CO_2/y (see Section 2.1) would require at least 11,335 plants, consuming in total 2.23 TW, or 19,534 TWh/y, of renewable electricity—roughly 73% of current global electricity generation by all means (26,619 TWh/y [9]). For the same 10 Gt/y removal rate, Carbon Engineering's natural gas-driven DAC process would require 58% of 2019's global natural gas production [9].

The task of Direct Air Capture of CO_2 at rates significant enough to have global impact (10 Gt/y) is tremendous, where even fully reversible systems would require large portions of the world's current power generation or natural gas production. At the desired rates of CO_2 removal [4], the use of DAC systems would have significant impact on the world's energy systems. It goes without saying that if DAC is to have a meaningful future, substantial improvements in process design and efficiency are vital.

Acknowledgements

We gratefully acknowledge support from the National Science and Engineering Research Council of Canada (NSERC, grant no. RGPIN-2016-03679).

We also thank the Pacific Institute for Climate Solutions (PICS), Ocean Networks Canada and the Solid Carbon team for their valuable input.

Declaration of Interests

The authors have no ownership stake in Carbon Engineering or any other organizations referenced as part of this publication. This analysis was performed independently using publicly available data from Carbon Engineering's whitepaper [1], where all usages were cited accordingly.

Chapter 3

Further Assessment of Calciner Improvements

3.1 Direct and Electric Heating

As discussed in Sections 2.4.6 and 2.6.2, while the largest losses to irreversibilities are owed to process chemistry, significant portions may be avoided if the plant configuration relying on natural gas is replaced with an all-electric one.

Section 2.6.4 discussed use of a theoretical, all-electric calciner. Based on a plant configuration which replaces the NGCC power island with renewable capacity, and given a capture rate of 111.9 t-CO_2/h, $CaCO_3$ pellet production would be reduced from 300 t/h [1] to ~261 t/h due to lack of additional CO_2 being produced by the NGCC system's gas turbine. With $CaCO_3$ decomposition requiring 166.2 kJ/mol at the calciner's operating temperature (900°C), a minimum thermal requirement of 117 MW was found for the all-electric plant's calciner, and with it a minimum work loss of 29.3 MW, though these values only accounted for heat consumed by the reaction itself.

Thus, for further analysis, the heating and cooling of incoming and outgoing flows must be examined, and with this the effects on thermal demand and work loss. To begin, we consider a calciner which directly receives its heat $\dot{Q}_{calc}$ from an arbitrary source, but does not introduce any new material flows as part of the heating process (Figure 3.1). We add a heat exchanger such that high-temperature outflows transfer heat to lower-temperature inflows, with no mixing effects being involved due to the presence of only one gaseous species (CO_2).

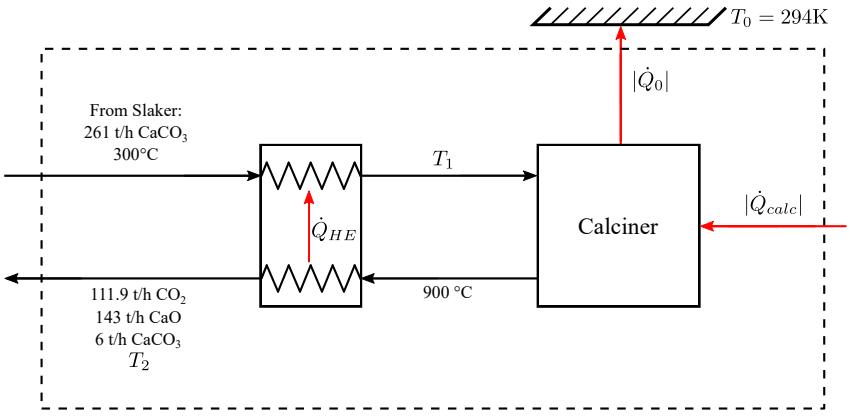

Figure 3.1: Directly-Heated Calciner System with Preheat Heat Exchanger

$CaCO_3$ pellets enter at a rate of 261 t/h, arriving from the slaker at 300°C. They receive heat $\dot{Q}_{HE}$ from the product outflow, and enter the calciner at temperature T_1. Within the calciner, 255 t/h of $CaCO_3$ are consumed in reaction to release 111.9 t/h of CO_2 with 143 t/h of CaO, and both leave with the unreacted

6 t/h flow of $CaCO_3$ at the calciner's operating temperature of 900°C. Finally, the hot product stream transfers heat to the incoming $CaCO_3$ pellets, and leaves the heat exchanger at temperature T_2. Note that the small flow of residual K_2CO_3, as was included in Figure 2.5, is neglected here due to it being largely uninvolved in the calciner's operation.

For analysis, we consider a calciner which dissipates no heat to the environment, i.e., $\dot{Q}_0 = 0$, and apply balance Eqs. (2.2) and (2.4) to the system shown. Figure 3.2(a) visualizes the relationship between overall calciner thermal demand $\dot{Q}_{calc}$ and the temperatures at which reactants and products leave the heat exchanger, while Figure 3.2(b) plots thermal demand and work loss/exergy destruction against heat exchanger effectiveness, defined as

$$\epsilon = \frac{\dot{Q}_{HE}^{act}}{\dot{Q}_{HE}^{max}}, \tag{3.1}$$

where $\dot{Q}_{HE}^{max}$ is the maximum possible heat exchange within the heat exchanger, and $\dot{Q}_{HE}^{act}$ is the actual heat exchange which takes place.

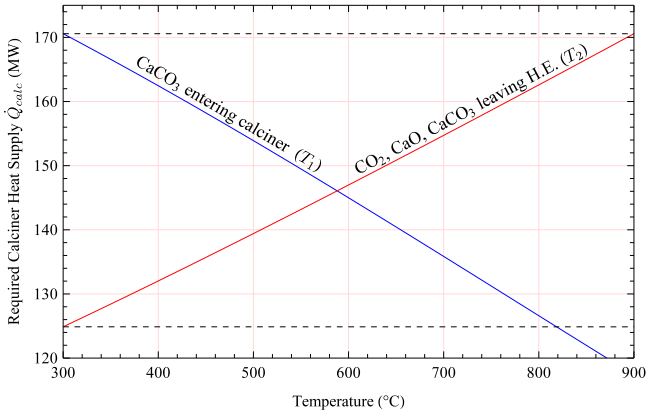

(a) Required Calciner Heat Supply and Incoming and Outgoing Flow Temperatures

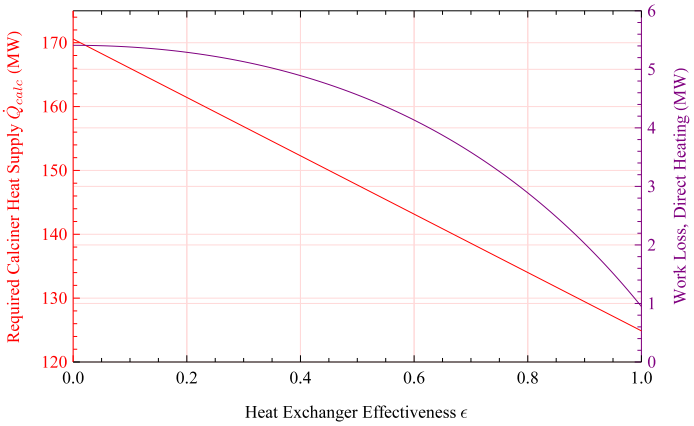

(b) Required Calciner Heat Supply, Heat Exchanger Effectiveness, and Work Loss for Direct Heating

Figure 3.2: Relationships between Calciner Heat Supply, Heat Exchange between Flows, and Work Loss for Direct Heating with No Heat Loss to the Environment

Figures 3.2(a) and 3.2(b) show that the minimum required heat supply for the calciner is 124.9 MW, corresponding to products leaving the heat exchanger at 300°C and $CaCO_3$ entering the calciner at 818.7°C ($\epsilon = 1$). Due to $CaCO_3$'s higher heat capacity, this represents perfect heat exchange, i.e., the maximum theoretical temperature to which incoming $CaCO_3$ pellets may be preheated, with the heat exchanger transferring heat over infinitesimal temperature differences. While it is unclear whether the slaker requires incoming pellets to be ~670°C as shown in Carbon Engineering's plant schematic (see Ref. [1]), for $T_2 = 677$°C, as obtained by energy balance in Section 2.4.1, the required heat supply becomes 152.9 MW, with effectiveness $\epsilon = 0.386$.

The importance of adequately preheating incoming $CaCO_3$ pellets using outgoing products is also made clear by Figure 3.2. Given the $CaCO_3$ reaction's enthalpy of reaction,

$$\triangle \bar{h}_R(900^\circ\text{C}, 1\text{ bar}) = 166.2\,\text{kJ/mol},$$

at least 117.4 MW of heat will always be required to react 255 t-$CaCO_3$/h. However, with the heat exchanger not present ($\epsilon = 0$), the minimum required heat supply becomes 170.6 MW, i.e., an additional 53.2 MW of provided heat must be dedicated solely to heating incoming $CaCO_3$ from 300°C to 900°C. By contrast, in the case of perfect heat exchange ($\epsilon = 1$), only 124.9 MW − 117.4 MW = 7.5 MW of additional heat is required, as the temperature of incoming pellets need only be raised from 818.7°C to 900°C.

Based on the results obtained, the general expression for the calciner's thermal demand reads

$$\dot{Q}_{calc} = \dot{Q}_{rxn} + \dot{Q}_{PH} + \dot{Q}_{loss}, \tag{3.2}$$

where

$$\dot{Q}_{rxn} = \dot{n}_{CaCO_3} \triangle \bar{h}_R(900^\circ\text{C}, 1\text{ bar}) \tag{3.3}$$

is owed to the chemical reaction,

$$\dot{Q}_{PH} = \dot{n}_{CaCO_3}\left[\bar{h}_{CaCO_3}(900^\circ\text{C}, 1\text{ bar}) - \bar{h}_{CaCO_3}(T_1, 1\text{ bar})\right] \tag{3.4}$$

is owed to heating incoming pellets by the temperature differential (900°C − T_1), and $\dot{Q}_{loss}$ represents heat loss to the environment by all enclosed system components in Figure 3.1. Thus, the ideal calciner will preheat incoming $CaCO_3$ as much as possible to minimize overall thermal demand $\dot{Q}_{calc}$.

To calculate work losses for the direct-heating case, Eq. (2.4) was applied over the system shown in Figure 3.1, taking the form

$$\dot{W}_{loss}^{calc,DH} = T_0 \dot{S}_{gen} = \sum_{in} \dot{n}_i(\bar{h}_i - T_0\bar{s}_i) - \sum_{out} \dot{n}_e(\bar{h}_e - T_0\bar{s}_e) + \left(1 - \frac{T_0}{T_{calc}}\right)\dot{Q}_{calc}, \tag{3.5}$$

where $T_{calc} = 1173.15$ K is the calciner's operating temperature. As shown by Figure 3.2(b), in comparison to the values obtained in Sections 2.4.1 and 2.6.4, exergy destruction is remarkably small when direct heating is used instead of a work resource. For the case of perfect preheater heat exchange ($\epsilon = 1$), the work loss becomes 0.948 MW, and in the absence of any heat exchange ($\epsilon = 0$), it reaches a maximum of 5.41 MW.

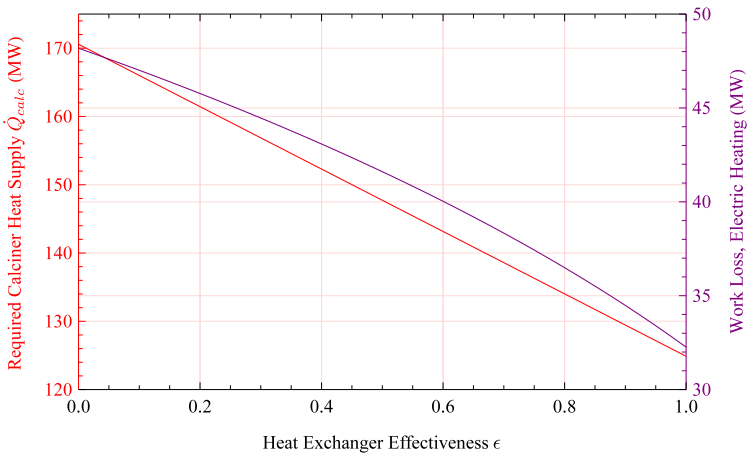

Figure 3.3: Required Calciner Heat Supply, Heat Exchanger Effectiveness, and Work Loss for Electric Heating

Figure 3.3 repeats Figure 3.2(b) for the case of electric resistance heating, or any heating process in which electrical energy is converted entirely to thermal energy, e.g., electric arc heating. With electrical power now being used, the Carnot factor $\left(1 - \frac{T_0}{T_{calc}}\right)$ vanishes from Eq. (3.5), and the power term

$$\dot{W}_{calc}^{elec} = \dot{Q}_{calc} \tag{3.6}$$

is added. Hence, the work loss equation takes the form

$$\dot{W}_{loss}^{calc,EH} = T_0 \dot{S}_{gen} = \sum_{in} \dot{n}_i (\bar{h}_i - T_0 \bar{s}_i) - \sum_{out} \dot{n}_e (\bar{h}_e - T_0 \bar{s}_e) + \dot{W}_{calc}^{elec}, \tag{3.7}$$

its resulting values being 32.3 MW for the case of perfect preheater heat exchange, 43.3 MW for CaO exiting at $T_2 = 677$°C, and 48.2 MW for no heat exchanger being present.

Note that for nonzero $\dot{Q}_{loss} = 6.6$ MW, as was found in Section 2.4.1, both $\dot{Q}_{calc}$ and $\dot{W}_{loss}^{calc,EH}$ values simply increase by 6.6 MW (see Eqs. (3.2, 3.6, 3.7). Additionally, while 29.3 MW was estimated in Section 2.6.4, the 32.3 MW value obtained here accounts for the remaining heat $\dot{Q}_{PH}$ to be transferred to incoming pellets to raise them from T_1 to 900°C. Hence, it can safely be considered the more accurate value of minimum work loss for an electric calciner.

Overall, the resulting values of work loss for electric heating are significantly larger than those obtained for direct heating. Solving Eqs. (3.5) and (3.7) for the difference gives

$$\dot{W}_{loss}^{calc,EH} - \dot{W}_{loss}^{calc,DH} = \dot{Q}_{calc} \left(\frac{T_0}{T_{calc}}\right), \tag{3.8}$$

i.e., the reduction in work loss for direct heating is owed to externalizing the conversion of power to heat from the calciner system. In doing so, the split between entropy generated in providing heat, and in consuming heat for chemical reaction and pellet heating, is made clear – heat addition to the calciner at 900°C from a high-temperature heat source accounts for 97% to 89% of total entropy generation in the electric calciner for the respective range of $\dot{Q}_{calc}$ values considered (124.9 MW to 170.6 MW), the latter percentage resulting from an increased share of entropy generation associated with heating $CaCO_3$ from 300°C to 900°C using provided heat.

Thus, the conversion of work to heat produces a significant loss which would not occur if heat were readily available from a high temperature source. Improvement therefore necessitates a means of using such a source which does not rely on electric power (which, after all, must be generated from renewables), and is easily accessible. The use of concentrated solar radiation may prove a productive route to explore, as has been tested by Esence et al. for small $CaCO_3$ mass flows [30], provided it may be effectively scaled to the large size required for the Carbon Engineering process.

While necessary rates of heating have been determined, the question remains of how the required amount of heat, or work, is to be provided to the calciner, i.e., the way the heat is to be delivered at high temperature to $CaCO_3$ pellets for reaction.

3.2 Electrically-Heated Calciner with Recirculating CO_2

Thus far, use of electric resistance heating to provide heat to the calciner has only been analyzed on the basis of energy requirements and work losses, though possible means of delivering the required heat to $CaCO_3$ pellets have yet to be explored in detail. This section examines use of an electrically-heated calciner using a recirculating flow of pure CO_2, stripped from the outgoing product stream, for pellet fluidization and as a heat transfer medium.

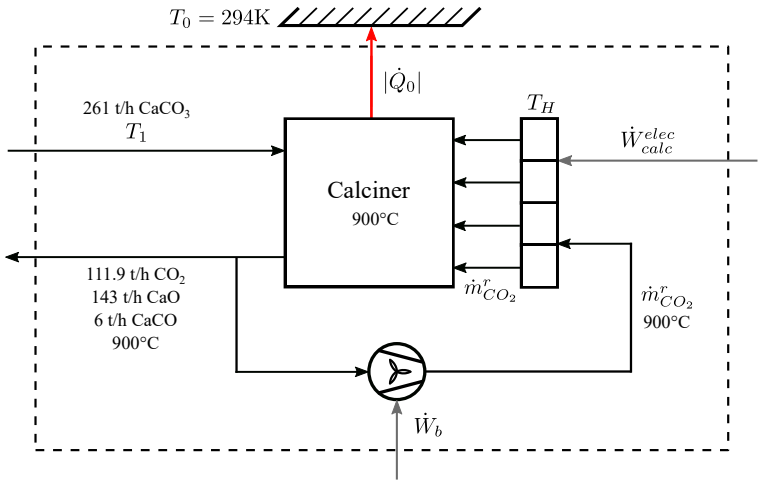

Figure 3.4: Process Schematic, Electrically-Heated Calciner with Recirculating CO_2

Figure 3.4 shows the proposed configuration to be analyzed. As in Section 3.1, a mass flow of 261 t/h of $CaCO_3$ enters the calciner at temperature T_1, while CO_2, CaO and residual $CaCO_3$ leave at 900°C. An additional mass flow of CO_2, denoted $\dot{m}^r_{CO_2}$, is stripped from the product stream to recirculate through the calciner after passing through a blower fan and heater. We ask for the minimum heater temperature T_H such that the required heat supply

$$\dot{Q}_{calc} = \dot{W}^{elec}_{calc}$$

may be delivered to the calciner through the convective flow of recirculating CO_2.

With the calciner treated as adiabatic ($\dot{Q}_0 = 0$) and fan/blower work $\dot{W}_b$ neglected for analysis purposes, applying the energy balance equation (2.2) to the calciner in Figure 3.4 results in the relationship

between minimum required heater temperature, recirculating CO_2 mass flow, and electrical power demand as shown in Figure 3.2. The three power demand values $\dot{W}^{elec}_{calc} = 170.6\,\text{MW}$, 152.9 MW and 124.9 MW were selected based on the discussion of Section 3.1, where their quantities correspond to incoming reactant temperatures $T_1 = 300°\text{C}$, 511°C, and 818.7°C, respectively.

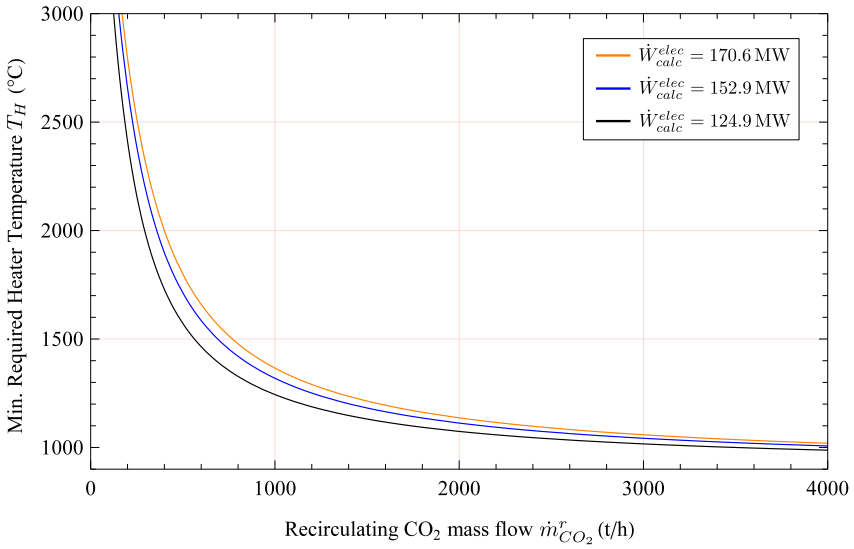

Figure 3.5: Minimum Required Heater Temperature as a function of Recirculating CO_2 Mass Flow for an Adiabatic, Electrically-Heated Calciner

As the mass flow of recirculating CO_2 $\dot{m}^r_{CO_2}$ decreases towards zero, the minimum heater temperature T_H increases towards infinity for fixed power input $\dot{W}^{elec}_{calc}$, as is expected – the smaller the mass (or mole) flow rate, the higher the enthalpy difference must be in incoming and outgoing CO_2 to deliver the constant amount of heat $\dot{Q}_{calc}$. Likewise, as the mass flow of recirculating CO_2 approaches infinity, the minimum heater temperature decreases towards the calciner's operating temperature (900°C).

However, for even the lowest calciner power demand, $\dot{W}^{elec}_{calc} = 124.9\,\text{MW}$, a trade-off between extreme heater temperature or massive recirculating mass flow perpetually exists, where in practice, heater temperature would need to be even higher than T_H such that a sufficient temperature difference exists for adequate heater-to-CO_2 heat transfer. A minimum heater temperature of 1000°C corresponds to a 3500 t/h flow of gaseous CO_2, or by volume, ~2308 m^3/s at a pressure of 1 bar. Processing this quantity of gas would likely be a considerable task, demanding at least a very physically large system with highly effective insulation to maintain the high temperatures, along with a large blower/fan system consuming large amounts of power.

Meanwhile, if the mass flow is reduced to 200 t/h of recirculating CO_2, a more manageable quantity, the minimum heater temperature required becomes 2412°C. With this temperature exceeding the melting point of most common materials, such a heater would need to be a highly engineered, specialty design, which may prove too cost-intensive.

Hence, the argument may be made that for the majority of combinations of heater temperature and recirculating mass flow, the heat capacity of CO_2 is too low to make it an effective carrier of thermal energy for the system depicted in Figure 3.4. If a balance is struck between the two, i.e., $T_H = 1387°\text{C}$ with $\dot{m}^r_{CO_2} = 700\,\text{t/h}$ for the more realistic $\dot{W}^{elec}_{calc} = 152.9\,\text{MW}$, the success of the system, while thermodynamically feasible, would ultimately depend on the costs of its construction, operation, and power

supply.

It should be recalled, however, that the values obtained for minimum heater temperature and recirculating mass flow depend on the heating requirement $\dot{Q}_{calc}$, which itself depends on the mole/mass flow rate and specific enthalpy change of incoming $CaCO_3$ (Eqns. (3.2), (3.3), (3.4)). Thus, if the mass flow rate of incoming $CaCO_3$ were reduced from 111.9 t/h, the required heater temperature and mass flow of recirculating CO_2 would decrease proportionally. Indeed, alternative configurations are certainly possible which may exploit this, i.e., use of several individual calciner configurations in parallel which exhaust CaO and CO_2 to a common outlet stream, or possibly use of a CO_2 stream which is heated and recirculated internally. The analysis of such configurations, as well as their detailed design, is left to future research.

Chapter 4

Net Work Loss for an All-Electric Plant

In Carbon Engineering's natural gas fuelled process, as was discussed in the research paper (Chapter 2), the net work loss was found to be 252 MW with respect to energy supplied, or 258 MW in total when accounting for exergy destroyed through water evaporation in the Air Contactor. The 252 MW value yielded a second-law efficiency of 7.8% for the plant, corresponding to ~13× more energy being consumed in practice compared to the theoretical, fully-reversible case (21.20 MW, Section 2.3.1).

As discussed in Section 2.6.2, use of a renewable power island would eliminate 17.3 t/h of additional CO_2, produced as a natural gas combustion product, from being introduced to the plant for processing, reducing necessary $CaCO_3$ production by 39 t/h. Combined with an electric calciner, a total of 54.1 t/h of additional CO_2 would be eliminated from the calciner's outgoing gas stream, reducing compression work by ~32%. The plant's power requirement, less that provided to the calciner to meet its thermal demand, would then total ~35 MW, assuming the compression system to require 14.8 MW to process 111.9 t-CO_2/h, the NGCC system's CO_2 Absorber to be removed, and all other components to require the same power input as found in Ref. [1].

Based on this data, as well as the estimates for calciner power requirements provided in Chapter 3, this section provides a more detailed analysis of net work loss for an all-electric plant configuration similar to what was done in Section 2.3.3, and with it an estimate for second-law efficiency.

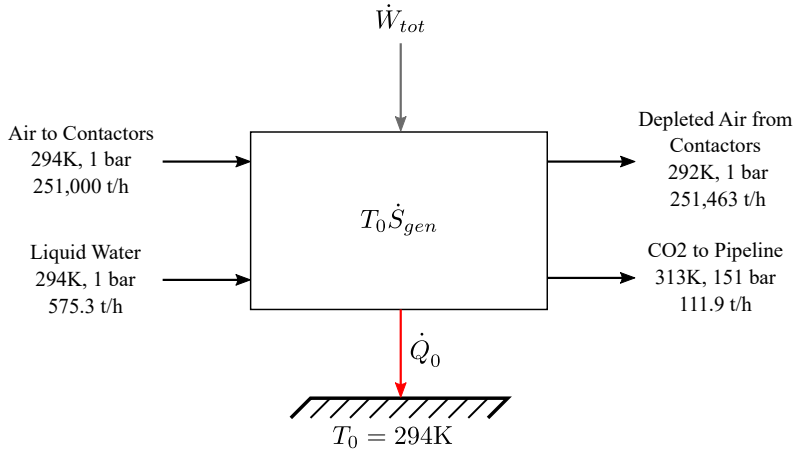

Figure 4.1: System-Level Flow Diagram of an All-Electric Plant

Figure 4.1 shows the all-electric configuration in question. Here, we assume the same incoming mass flow to the air contactor: 251,000 t/h of air consisting of 0.06% CO_2, 23.00% O_2, 75.96% N_2 and 0.98% H_2O by mass [1].

In contrast to the natural gas configuration of Figure 2.3, an additional 44.3 t/h is added to the incoming liquid water stream for a total water inflow of 575.3 t/h. This additional water replaces the same amount previously produced through combustion within the plant, eventually finding its way to the Air Contactor's KOH solution after the water knockout and pellet washing stages. Maintaining an

identical amount of water allows for the assumption that the Air Contactor's thermochemical behavior remains largely unchanged in the all-electric configuration, hence allowing the depleted air stream to be assumed leaving at roughly the same temperature as in the natural gas configuration (19°C) due to evaporative cooling.

As has been discussed, with no combustion taking place, no additional CO_2 is introduced within the plant. Thus, the compression system processes 111.9 t/h of pure CO_2, where an exit temperature of 40°C (313 K) is assumed, as was used before.

Finally, we introduce the work quantity $\dot{W}_{tot}$ to represent the total electrical power input to the all-electric plant, expressed as

$$\dot{W}_{tot} = \dot{W}_{PI} + \dot{W}^{elec}_{calc}, \tag{4.1}$$

where $\dot{W}^{elec}_{calc}$ represents the required power input to the calciner to meet its thermal demand (Chapter 3), and $\dot{W}_{PI}$ the 35 MW of power demanded by remaining plant components.

Assuming the calciner loses the same amount of heat $|\dot{Q}_0| = 6.6\,\text{MW}$ to the environment as found in Section 2.4.1, and with its product stream assumed leaving to the slaker at 677°C (Figure 2.5), the power requirement $\dot{W}^{elec}_{calc} = 159.5\,\text{MW}$ is found using the results of Section 3.1. Thus, the plant's total electrical power requirement is found as

$$\dot{W}_{tot} = \dot{W}_{PI} + \dot{W}^{elec}_{calc} = 35\,\text{MW} + 159.5\,\text{MW} = 194.5\,\text{MW}.$$

Appying Eq. (2.4) over the entirety of the all-electric plant results in the net work loss to entropy generation

$$\dot{W}^{tot}_{loss} = 180.5\,\text{MW},$$

where, together with the 21.20MW reversible work requirement for separation and compression of 111.9 t-CO_2/h (Section 2.3.1), we find

$$\dot{W}^{tot}_{loss} + |\dot{W}^{tot}_{rev}| = 201.7\,\text{MW}$$

as the total work potential consumed by the all-electric plant.

As was seen in the similar analysis of Section 2.3.3 for the natural gas configuration, the value of total work potential consumed (201.7 MW) is deceptively higher than the total power requirement $\dot{W}_{tot} = 194.5\,\text{MW}$, implying the net work loss $\dot{W}^{tot}_{loss}$ exceeds its intuitively expected value by 7.2 MW. However, this is again attributable to evaporation of water in the Air Contactor.

To more adequately explain this phenomenon, we consider a system which adds the same mass flow of liquid water to an identical incoming air stream, the only outflow being a mixture of air and water vapor. We ask for the reversible work obtained in evaporating all incoming liquid.

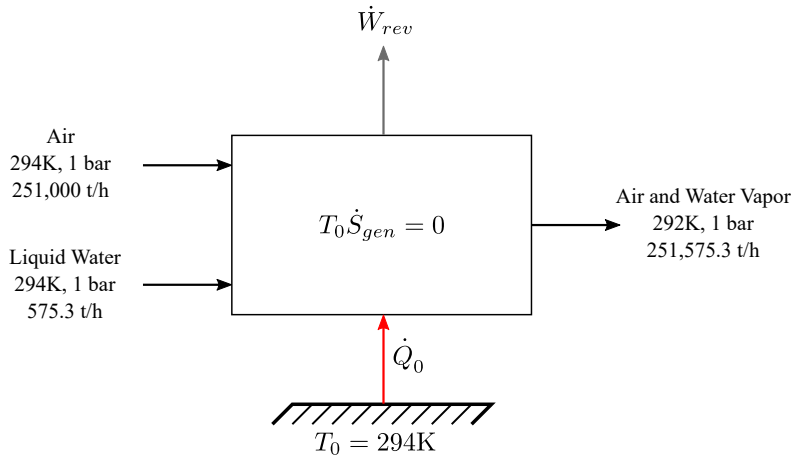

Figure 4.2: Reversible Evaporation of Liquid Water into an Air Stream

Applying Eqs. (2.4) and (2.2) to the system of Figure 4.2, we find the heat $\dot{Q}_0 = 249\,\text{MW}$ and the reversible work $\dot{W}_{rev} = 7.4\,\text{MW}$, i.e., the theoretical maximum available work from evaporating incoming water into the air stream. This value is remarkably close to the 7.2 MW of additional work loss mentioned above, the difference being mainly attributable to differing mass flows of outgoing air.

Though the all-electric plant indeed sees a similar value for theoretical work available from evaporation, in practice it cannot be harnessed as useful power. Thus, it is an instance of destroyed exergy, hence its contribution to the net work loss $\dot{W}_{loss}^{tot}$.

Once again, this loss of work potential owed to evaporation cannot be considered meaningful in the context of the process' evaluation, as the evaporation draws thermal energy from the environment as opposed to the plant's energy source. Thus, we define the additional quantity

$$\dot{W}_{loss}^{elec} = 180.5\,\text{MW} - 7.2\,\text{MW} = 173.3\,\text{MW}$$

as the net loss of work potential with respect to electrical power provided, where 49.9 MW (28.8%) is attributable to the calciner.

Using this value with the reversible work requirement (21.20 MW) in Eq. (2.7) gives a second-law efficiency estimate of

$$\eta_{II} = 0.11 = 11\%$$

for an all-electric plant configuration with CO_2 compression to 151 bar, an improvement of 3.2% compared to the natural gas-fuelled plant as assessed in Section 2.3.3.

While only a minor improvement from a second-law perspective, the all-electric configuration discussed indeed reduces the plant's net power demand by 78.7 MW, the key mechanisms being the reduction of $CaCO_3$ production, and hence calciner thermal demand, to process the NGCC system's exhaust, the compression system's decreased power demand owed to elimination of natural gas-produced CO_2, and elimination of the need for an ASU and water knockout system. An additional advantage worth considering is elimination of the potential for upstream fugitive methane emissions which, if present, would severely hamper the DAC plant's value proposition as a net-negative technology.

Thus, while we leave detailed techno-economic analysis to future research, it may be safely concluded that an all-electric plant configuration powered by renewable energy would be a productive improvement to explore with regard to net energy consumption.

Summary and Conclusions

This thesis presents a thermodynamic loss analysis for Carbon Engineering's 1 Mt-CO_2/year Direct Air Capture plant, with further analysis and discussion on means to improve its energy efficiency.

Results indicate that the largest losses of work potential in their plant occur due to chemical exergy dissipation, i.e., rejection of heat near ambient temperature to the environment through exothermic chemical reactions. While these losses are largely unavoidable, being a product of the chemical looping steps at the heart of the plant's design, other losses, primarily associated with use of natural gas for power and calcination, may be reduced without significantly altering process chemistry.

While the calciner's thermal demand depends on the quantity of $CaCO_3$ it processes, it is also heavily driven by the degree to which its incoming and outgoing flows exchange heat. A calciner heated through electric resistance heating, as part of an all-electric plant configuration, would require at minimum 124.9 MW of heat input, corresponding to incoming $CaCO_3$ pellets reaching their highest theoretical preheat temperature of 818.7°C. In absence of preheating, an additional 45.7 MW of heat input would be required, a thermal demand increase of ~37%. While in reality, preheater heat exchange effectiveness ϵ will indeed be less than unity, adequate preheating and insulation against heat loss is critical for a thermally efficient calciner system.

As was revealed by second-law analysis, 89% - 97% of an electric calciner's entropy generation would result from the conversion of work into heat. In other words, considering a renewable system as the power source, e.g. solar photovoltaic with appropriate storage capacity, a large loss would result from the conversion of power to heat, in addition to the loss in converting solar radiation to power, due to limited energy conversion efficiency. If heat were readily available from a high-temperature source, i.e., if concentrated solar radiation were used directly, the determined 32.3 to 48.2 MW loss of incoming work potential would be reduced to between 0.948 and 5.41 MW. The question remains, however, of how this may be practically implemented.

Should a work resource be directly used for calcining, as is the case for electric heating, the mechanism by which heat is delivered to $CaCO_3$ pellets must be carefully considered. Section 3.2 analyzed use of recirculating CO_2 as a convective flow to deliver heat generated through electric resistance, though prohibitively high heater temperatures and/or mass flows would result if the configuration considered (Figure 3.4) were used. However, alternative configurations which treat smaller mass flows of $CaCO_3$, such as separate calciners operating in parallel, or use of internal heating and CO_2 circulation, may abate this problem. Their investigation is left to future research.

Finally, a total power input of 194.5 MW is estimated for an all-electric plant configuration, resulting in a marginal increase of the plant's second-law efficiency by 3.2%. While this indeed realizes reductions of 78.7 MW to both energy demand and work loss, they may not be substantial enough to justify installation and use of heavy renewable capacity [29] solely as a DAC power source. Instead, this capacity may be better used in replacing fossil fuel power generation directly.

Overall, development of technologies for large-scale atmospheric CO_2 removal must be encouraged given the strictly limited time available to address the global climate problem. For the rates of atmospheric CO_2 removal necessary [6], even with the suggested improvements implemented, Carbon Engineering's process at present consumes prohibitively large amounts of energy to be considered in a state of technological readiness. Given the extraordinary amounts of energy demanded by even fully reversible DAC systems for removal of 10 gigatons of atmospheric CO_2 per year, an immense amount of future work remains to make Direct Air Capture a viable option for climate change mitigation.

Bibliography

[1] D. W. Keith, G. Holmes, D. S. Angelo, and K. Heidel, "A Process for Capturing CO2 from the Atmosphere," *Joule*, vol. 2, no. 8, pp. 1573–1594, 2018.

[2] Dlugokencky, E.J. and Mund, J.W. and Crotwell, A.M. and Thoning, K.W., "Atmospheric Carbon Dioxide Dry Air Mole Fractions from the NOAA GML Carbon Cycle Cooperative Global Air Sampling Network, 1968-2020, Version: 2021-07-30," 2021.

[3] P. Tans and R. Keeling, "Trends in Atmospheric Carbon Dioxide," N. O. A. A. Global Monitoring Laboratory. [Online]. Available: https://www.esrl.noaa.gov/gmd/ccgg/trends/monthly.html

[4] J. Rogelj, D. Shindell, K. Jiang, S. Fifita, P. Forster, V. Ginzburg, C. Handa, H. Kheshgi, S. Kobayashi, E. Kriegler, L. Mundaca, R. Séférian, M. V. Vilarino, K. Calvin, J. C. de Oliveira de Portugal Pereira, O. Edelenbosch, J. Emmerling, S. Fuss, T. Gasser, N. Gillett, C. He, E. Hertwich, L. Höglund-Isaksson, D. Huppmann, G. Luderer, A. Markandya, M. Meinshausen, D. McCollum, R. Millar, A. Popp, P. Purohit, K. Riahi, A. Ribes, H. Saunders, C. Schädel, C. Smith, P. Smith, E. Trutnevyte, Y. Xu, W. Zhou, and K. Zickfeld, "Mitigation Pathways Compatible with 1.5°C in the Context of Sustainable Development," in *Global warming of 1.5°C. An IPCC Special Report on the impacts of global warming of 1.5°C above pre-industrial levels and related global greenhouse gas emission pathways, in the context of strengthening the global response to the threat of climate change, sustainable development, and efforts to eradicate poverty*, ser. IPCC Special Report, V. Masson-Delmotte, P. Zhai, H. O. Pörtner, D. Roberts, J. Skea, P. R. Shukla, A. Pirani, W. Moufouma-Okia, C. Péan, R. Pidcock, S. Connors, J. B. R. Matthews, Y. Chen, X. Zhou, M. I. Zhou, E. Lonnoy, T. Maycock, M. Tignor, and T. Waterfield, Eds. Geneva: Intergovernmental Panel on Climate Change, 2018, ch. 2, pp. 93–174.

[5] A. Bergman and A. Rinberg, "The case for carbon dioxide removal: From science to justice," in *CDR Primer*, J. Wilcox, B. Kolosz, and J. Freeman, Eds., 2021, ch. 1.

[6] The National Academies of Sciences, Engineering and Medicine, *Negative Emissions Technologies and Reliable Sequestration: A Research Agenda*. Washington, DC: The National Academies Press, 2019.

[7] K. Heidel, D. Keith, A. Singh, and G. Holmes, "Process design and costing of an air-contactor for air-capture," *Energy Procedia*, vol. 4, pp. 2861–2868, 2011.

[8] A. I. Osman, M. Hefny, M. I. A. A. Maksoud, A. M. Elgarahy, and D. W. Rooney, "Recent advances in carbon capture storage and utilisation technologies: a review," *Environmental Chemistry Letters*, vol. 19, no. 2, pp. 797–849, 2020.

[9] IEA, "Key World Energy Statistics 2020," 2020. [Online]. Available: https://www.iea.org/reports/key-world-energy-statistics-2020

[10] R. Long-Innes and H. Struchtrup, "Thermodynamic loss analysis of a liquid-sorbent direct air carbon capture plant," Submitted to *Cell Reports Physical Science*, 2021.

[11] "Paris Agreement to the United Nations Framework Convention on Climate Change," adopted 12. Dec 2015, entered into force 4 Nov. 2016, United Nations Treaty Collection, Chapter XXVII-7.d.

[12] The World Bank, "Consumer price index (2010 = 100) - United States." [Online]. Available: https://data.worldbank.org/indicator/FP.CPI.TOTL?locations=US

[13] The World Bank, "GDP (Constant 2010 US$)." [Online]. Available: https://data.worldbank.org/indicator/NY.GDP.MKTP.KD

[14] P. J. Linstrom and W. G. Mallard, *NIST Chemistry WebBook, NIST Standard Reference Database 69*. Gaithersburg, MD: National Institute of Standards and Technology, 1997.

[15] G. K. Jacobs, D. M. Kerrick, and K. M. Krupka, "The high-temperature heat capacity of natural calcite (CaCO3)," *Physics and Chemistry of Minerals*, vol. 7, no. 2, pp. 55–59, 1981.

[16] Y. Cengel and M. Boles, *Thermodynamics: An Engineering Approach*, 9th ed. New York, NY: McGraw-Hill, 2019.

[17] International Association for the Properties of Water and Steam, "Revised Release on the IAPWS Industrial Formulation 1997 for the Thermodynamic Properties of Water and Steam," Lucerne, Switzerland, 2007.

[18] R. Span and W. Wagner, "A New Equation of State for Carbon Dioxide Covering the Fluid Region from the Triple-Point Temperature to 1100 K at Pressures up to 800 MPa," *Journal of Physical and Chemical Reference Data*, vol. 25, no. 6, pp. 1509–1596, 1996.

[19] H. Struchtrup, *Thermodynamics and Energy Conversion*, 1st ed. Springer-Verlag Berlin Heidelberg, 2014.

[20] H. J. Herzog, "What future for carbon capture and sequestration?" *Environmental Science & Technology*, vol. 35, no. 7, pp. 148–153, 2001.

[21] H. S. Caram, R. Gupta, H. Thomann, F. Ni, S. C. Weston, and M. Afeworki, "A simple thermodynamic tool for assessing energy requirements for carbon capture using solid or liquid sorbents," *International Journal of Greenhouse Gas Control*, vol. 97, p. 102986, 2020.

[22] N. McQueen, K. V. Gomes, C. McCormick, K. Blumanthal, M. Pisciotta, and J. Wilcox, "A review of direct air capture (DAC): scaling up commercial technologies and innovating for the future," *Progress in Energy*, vol. 3, no. 3, p. 032001, 2021.

[23] F. Sabatino, A. Grimm, F. Gallucci, M. v. S. Annaland, G. J. Kramer, and M. Gazzani, "A comparative energy and costs assessment and optimization for direct air capture technologies," *Joule*, vol. 5, no. 8, pp. 2047–2076, 2021.

[24] L. M. Romeo, I. Bolea, L. Yolanda, and J. M. Escosa, "Optimization of intercooling compression in CO2 capture systems," *Applied Thermal Engineering*, vol. 29, no. 8-9, pp. 1744–1751, 2009.

[25] D. H. Van Wagener, "Stripper modeling for CO2 removal using monoethanolamine and piperazine solvents," Doctoral Dissertation, University of Texas, Austin, Texas, USA, 2011.

[26] General Electric Company, "GEA34340 LM2500 Power Plants 60Hz FS," 2021. [Online]. Available: https://www.ge.com/content/dam/gepower-new/global/en_US/downloads/gas-new-site/products/gas-turbines/lm2500-60hz-fact-sheet-product-specifications.pdf

[27] S. Ó. Snæbjörnsdóttir, B. Sigfússon, C. Marieni, D. Goldberg, S. R. Gislason, and E. H. Oelkers, "Carbon dioxide storage through mineral carbonation," *Nature Reviews Earth & Environment*, vol. 1, no. 2, pp. 90–102, 2020.

[28] Thyssenkrupp Industrial Solutions, "Hydrogen from large-scale electrolysis: Efficient solutions for sustainable chemicals and energy storage," 2020. [Online]. Available: https://d2zo35mdb530wx.cloudfront.net/_binary/UCPthyssenkruppBAISUhdeChlorineEngineers/en/products/water-electrolysis-hydrogen-production/alkaline-water-electrolysis/link-thyssenkrupp_Hydrogen_Water_Electrolysis_and_green_chemicals.pdf

[29] N. McQueen, M. J. Desmond, R. H. Socolow, P. Psarras, and J. Wilcox, "Natural Gas vs. Electricity for Solvent-Based Direct Air Capture," *Frontiers in Climate*, vol. 2, p. 38, 2021.

[30] T. Esence, E. Guillot, M. Tessonneaud, J.-L. Sans, and G. Flamant, "Solar calcination at pilot scale in a continuous flow multistage horizontal fluidized bed," *Solar Energy*, vol. 207, pp. 367–378, 2020.